Title

Asymmetric transverse momentum broadening in an inhomogeneous medium

Journal

Physical Review D, 107(5)

ISSN

2470-0010

Authors

Fu, Yu

Casalderrey-Solana, Jorge

Wang, Xin-Nian

Publication Date

2023-03-01

DOI

10.1103/physrevd.107.054038

Asymmetric transverse momentum broadening in an inhomogeneous medium

Yu Fu,[1] Jorge Casalderrey-Solana,[2] and Xin-Nian Wang[1,3,*]

[1]*Key Laboratory of Quark and Lepton Physics (MOE) & Institute of Particle Physics, Central China Normal University, Wuhan 430079, China*

[2]*Departament de Física Quàntica i Astrofísica & Institut de Ciències del Cosmos (ICC), Universitat de Barcelona, Martí i Franquès 1, 08028 Barcelona, Spain*

[3]*Nuclear Science Division, Lawrence Berkeley National Laboratory, Berkeley, California 94720, USA*

(Received 18 April 2022; accepted 1 March 2023; published 28 March 2023)

Gradient jet tomography in high-energy heavy-ion collisions utilizes the asymmetric transverse momentum broadening of a propagating parton in an inhomogeneous medium. Such broadening is studied within a path-integral description of the evolution of the Wigner distribution for a propagating parton in medium. Going beyond the eikonal approximation of multiple scattering, the evolution operator in the transverse direction can be expressed as the functional integration over all classical trajectories of a massive particle with the light-cone momentum ω as its mass. With a dipole approximation of the Wilson line correlation function, evolution with the light-cone time t is determined by the jet transport coefficient $\hat{q}$ that can vary with space and time. In a uniform medium with a constant $\hat{q}_0$, the analytical solution to the Wigner distribution becomes a typical drifted Gaussian in both transverse momentum and coordinate with the diffusion width $\sqrt{\hat{q}_0 t}$ and $\sqrt{\hat{q}_0 t^3/3\omega^2}$, respectively. In the case of a simple Gaussian-like transverse inhomogeneity with a spatial width σ on top of a uniform medium, the final asymmetrical momentum distribution can be calculated semianalytically. The transverse asymmetry defined for jet gradient tomography that characterizes the asymmetrical distribution is found to linearly correlate with the initial transverse position of the propagating parton within the domain of the inhomogeneity. It decreases with the parton energy ω, increases with the propagation time initially and saturates when the diffusion distance is much larger than the size of the inhomogeneity or $t^3 \gg 3\omega^2\sigma^2/\hat{q}_0$. The transverse momentum broadening due to the inhomogeneity also saturates at late times in contrast to the continued increase with time if the drifted diffusion in space is ignored.

DOI: 10.1103/PhysRevD.107.054038

I. INTRODUCTION

A jet is essentially a collection of collimated showers of particles stemming from the fragmentation of energetic partons in high-energy hadron and nuclear collisions. In high-energy heavy-ion collisions, jets also interact with quark-gluon plasma (QGP), a deconfined and strongly coupled state of matter formed in the collisions [1–4], as they travel through the hot and dense matter. The final jet observables therefore should carry the information of jet-medium interactions and are naturally a useful probe of the fundamental properties of QGP.

When jets propagate through the strongly coupled QGP, the energetic partons undergo multiple scattering with the constituents of the QGP and lose their energy, giving rise to the strong attenuation of the high-transverse-momentum tails of single inclusive hadron spectra as well as the single inclusive jet spectra. These phenomena are usually referred to as jet quenching [5,6], which has been observed in experiments at the Relativistic Heavy-ion Collider (RHIC) via suppression of large-transverse-momentum (p_T) hadrons [7,8] and later confirmed at the Large Hadron Collider (LHC) via the dijet and γ/Z-jet asymmetry [9,10] and the suppression of high-p_T particles [11] and jets [12,13]. These experimental data have provided important information about the properties of the QGP through jet tomographic studies.

Central to the jet tomography is the energy loss and transverse momentum broadening of a propagating parton inside QGP. Following the first attempt to calculate the parton energy loss in QGP [14], several approaches have been established, including BDMPS-Z [15–20],

*xnwang@lbl.gov

GLV [21,22], ASW [23–27], AMY [28–30], and Higher-twist [31,32]. In these approaches, the parton energy loss is dictated by the jet transport coefficient $\hat{q}$, which is defined as the averaged transverse momentum broadening squared per unit length [16]. It has been extracted from comparisons between model calculations and experimental data on single inclusive hadron spectra at both the RHIC and LHC [33–35].

The initial jet production positions in high-energy nucleus-nucleus collisions in these model calculations are assumed to follow the number of binary nucleon-nucleon collisions with the Woods-Saxon nuclear distribution [36]. The final hadron spectra are averaged over the initial jet production positions and propagation direction. For non-central nucleus-nucleus collisions, the parton propagation length and energy loss will depend on the azimuthal angle of the initial parton propagation direction relative to the reaction plane. This will lead to the azimuthal anisotropy of the final hadron and jet spectra [37–39] which in turn can provide information about the path-length dependence of the parton energy loss and the geometrical properties of the QGP [40–46]. One can further use both longitudinal [47,48] and transverse jet tomography [49] to localize the initial jet production positions and study the space-time profile of the jet transport coefficient in more detail.

The longitudinal jet tomography utilizes the path-length dependence of the parton energy loss and suppression of the final hadron and jet spectra, while the transverse jet tomography relies on the asymmetrical transverse momentum broadening of the propagating parton due to the inhomogeneity of the jet transport coefficient in the transverse plane. The latter is also referred to as the gradient jet tomography. It has been applied to localize the initial transverse production positions of Z/γ jets to enhance the effect of the diffusion wake induced by Z/γ jets in the final Z/γ-hadron and jet-hadron correlations [50].

The principle of gradient jet tomography [49] is based on the asymmetrical transverse momentum broadening for an energetic parton propagating in a medium that is inhomogeneous in the transverse direction as characterized by the finite transverse gradient in the jet transport coefficient $\hat{q}$. One can study the asymmetrical transverse momentum broadening via solving a drift-diffusion Boltzmann equation which describes the diffusion of a jet parton in both transverse momentum and coordinate. The finite transverse gradient of the jet transport coefficient in a nonuniform medium leads to a drift in both the final transverse momentum and coordinate distribution of the jet parton which depends on the propagation length and the initial transverse position in the region of the medium with a finite gradient of the jet transport coefficient [49]. One can therefore use the transverse momentum asymmetry of the final jet particles to localize the initial transverse position of the jet production. This principle of gradient tomography has been verified [49] by full event-by-event simulations of γ-jet propagation within the linear Boltzmann transport model [51–54]. It has also been applied to the study of diffusion wakes induced by γ/Z jets in high-energy heavy-ion collisions [50].

In this study we formulate the transverse diffusion of a propagating parton in the path-integral approach [19,20,24,25] for the evolution of parton distributions which are defined via a Wigner function [55,56]. We illustrate the principle of the gradient tomography within the path-integral approach in a static medium which is uniform in the direction of the parton propagation but inhomogeneous in the transverse direction. Within a picture of multiple soft scatterings off independent scattering centers without color flow, the evolution of the Wigner function can be described by the Green function in QCD in a medium that is nonuniform in the transverse plane. One can express the final parton transverse momentum spectrum in terms of the Green function and calculate the transverse momentum asymmetry and study its path length and transverse gradient dependence. Both our approach with path integrals and the drift-diffusion Boltzmann equation assume the dominance of multiple soft scattering in the medium. However, the path-integral approach takes into account the quantum corrections due to fluctuations of the propagation path as compared to the semiclassical Boltzmann transport approach. Asymmetrical transverse momentum broadening due to multiple scatterings with the Gyulassy-Wang static potential model [14] in an inhomogeneous medium has also been studied recently in Refs. [57,58], taking into account the first transverse gradient correction. This first gradient correction is shown to satisfy a Boltzmann diffusion equation with a spatially dependent jet transport coefficient $\hat{q}$ [59]. The second-order gradient correction, however, gives rise to a novel term in the transport equation due to nonlocal interactions. In our path-integral approach here, we consider multiple scatterings with the dipole (or harmonic) approximation of the interaction but without gradient expansion in the formulation. We will consider, however, the linear gradient correction for an example of numerical calculations at the end.

The remainder of this paper is organized as follows. In Sec. II, we briefly review the Wilson line and the Green function or evolution operator for a parton traveling through a background medium within the multiple soft scattering picture. We introduce the Wigner function to describe the phase-space distribution of the parton projectile and employ the dipole approximation to relate the Wilson line correlations to the jet transport coefficient. We derive the final phase-space distribution of the propagating parton within the path-integral approach. In Sec. III, we derive the final phase-space distribution of a propagating parton in a uniform medium which is shown to satisfy the drift-diffusion Boltzmann equation. In Sec. IV, we calculate the final transverse momentum spectrum, transverse momentum broadening, and the transverse momentum

asymmetry of a jet parton propagating in a medium with a simple form of a transversely inhomogeneous jet transport coefficient. We examine their dependence on the initial transverse position, propagation length, and the energy. In Sec. V, we summarize the result.

II. PROPAGATION OF PARTONS IN MEDIUM

We consider a quark, starting from $x^+ = -\infty$, that propagates through a slab of medium that extends from x_0^+ to x_f^+ and continues to $x^+ = \infty$, as illustrated in Fig. 1. In the following, we denote the average transverse coordinates of the parton as $\boldsymbol{X}$ and $\boldsymbol{Y}$, while $\boldsymbol{x}$ and $\boldsymbol{y}$ are the fluctuations of the transverse coordinates with the corresponding conjugate transverse momenta $\boldsymbol{p}_0$ and $\boldsymbol{p}$.

To describe the propagation of an energetic parton in a QGP medium within the path-integral approach, we consider multiple soft interactions between a propagating quark and the background field $A(\boldsymbol{x}, x^+)$ of the QGP medium.[1] Here we adopt the light-cone variables for space-time coordinates,

$$x^{\pm} \equiv \frac{1}{\sqrt{2}}(t \pm z), \tag{1}$$

and similarly for other four-vectors. Here t is the time component and z is the longitudinal component (along the initial parton propagation direction) of the space-time four-vector. The transverse component is denoted by $\boldsymbol{x}$. Similarly, the light-cone momentum is p^+ and the transverse momentum is $\boldsymbol{p}$.

Assuming that the initial and final momentum of the quark are p and p', respectively, and p^+ is the large component of the momentum, these multiple soft interactions, as illustrated in Fig. 2, can be resummed under the eikonal approximation to give the S matrix [24,25,60–62],

$$S(p', p) \approx 2\pi\delta(p'^+ - p^+)2p^+ \times \int \mathrm{d}\boldsymbol{x} e^{-i(\boldsymbol{p}'-\boldsymbol{p})\cdot\boldsymbol{x}} W_{\parallel}(\boldsymbol{x}, x_0^+, x_f^+), \tag{2}$$

where the Wilson line in a covariant gauge is defined as

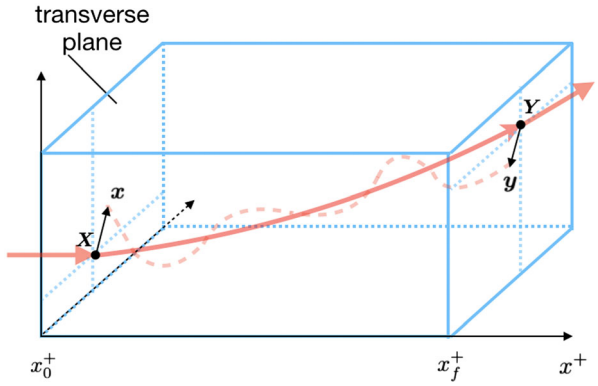

FIG. 1. Propagation of a quark through a slab of dense medium that extends from x_0^+ to x_f^+ on the light cone with the corresponding average transverse coordinate $\boldsymbol{X}$, $\boldsymbol{Y}$ and the fluctuations of the transverse coordinates $\boldsymbol{x}$ and $\boldsymbol{y}$.

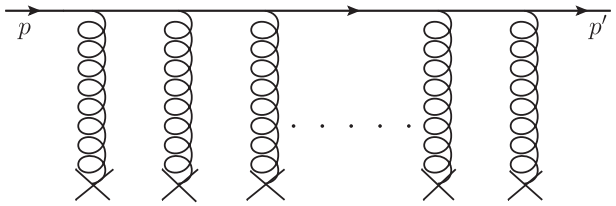

FIG. 2. Illustration of the eikonal propagation of a quark with initial momentum p and final momentum p' in the medium, where the X's donate the medium field.

$$W_{\parallel}(\boldsymbol{x}, x_0^+, x_f^+) = \mathcal{P}\exp\left[ig\int_{x_0^+}^{x_f^+} \mathrm{d}\xi^+ A^-(\boldsymbol{x}, \xi^+)\right], \tag{3}$$

and $\mathcal{P}$ denotes the path ordering of the field $A^-(\boldsymbol{x}, x^+)$.[2]

In the above eikonal approximation, the subleading term $p_\perp^2$ in poles of the propagator is ignored. To relax the eikonal approximation, we can keep the $p_\perp^2$ terms. This is equivalent to considering the Brownian motion of the propagating quark in the transverse plane. In this case, assuming that the initial and final coordinates are $(x_0^+, \boldsymbol{x}_0)$ and $(x_f^+, \boldsymbol{x}_f)$, respectively, the S matrix can be expressed in the path-integral form [24,25,60–62],

$$S(p', p) \approx 2\pi\delta(p'^+ - p^+)2p^+ \int \mathrm{d}\boldsymbol{x}_0 \mathrm{d}\boldsymbol{x}_f e^{i\boldsymbol{p}\cdot\boldsymbol{x}_0} e^{-i\boldsymbol{p}'\cdot\boldsymbol{x}_f} U_{\parallel}(\boldsymbol{x}_f, x_f^+; \boldsymbol{x}_0, x_0^+), \tag{4}$$

where

$$U_{\parallel}(\boldsymbol{x}_f, x_f^+; \boldsymbol{x}_0, x_0^+) = \int_{\boldsymbol{r}(x_0^+)=\boldsymbol{x}_0}^{\boldsymbol{r}(x_f^+)=\boldsymbol{x}_f} \mathcal{D}\boldsymbol{r}(x^+) \exp\left[i\frac{p^+}{2}\int_{x_0^+}^{x_f^+} \mathrm{d}x^+ \left(\frac{d\boldsymbol{r}}{dx^+}\right)^2\right] W_{\parallel}(\boldsymbol{r}, x_0^+, x_f^+), \tag{5}$$

[1]Herein, a bold letter denotes that the vector lies in the transverse plane.

[2]We exclude the fluctuation of the gauge field in the vacuum and only consider the effect of the medium.

is the Green function or evolution operator [24] that replaces the Wilson line in Eq. (2) and describes the quark's propagation in the transverse plane of the medium. In the adjoint representation, a similar expression for the propagation of a fast gluon with multiple soft scatterings was also derived in Ref. [60].

We use the gauge-invariant Wigner function [55,56],

$$\mathcal{W}(\boldsymbol{X},\boldsymbol{p};x_0^+,x^+)=\int \mathrm{d}^2\boldsymbol{x}e^{-i\boldsymbol{p}\cdot\boldsymbol{x}}\Psi\left(\boldsymbol{X}+\frac{\boldsymbol{x}}{2},x_0^+,x^+\right)\times\Psi^*\left(\boldsymbol{X}-\frac{\boldsymbol{x}}{2},x_0^+,x^+\right), \tag{6}$$

$$\Psi(\boldsymbol{x},x^+)=\psi(\boldsymbol{x},x^+)W_\parallel(\boldsymbol{x},x_0^+,x^+), \tag{7}$$

to describe the transverse phase-space distribution of a propagating quark at a given time x^+. The quark wave function $\Psi(\boldsymbol{x},x_0^+,x^+)$ with the insertion of the Wilson line $W_\parallel(\boldsymbol{x},x_0^+,x^+)$ is gauge invariant.

Using the evolution operator we can express the evolution of the gauge-invariant Wigner function at a later time x_f^+ from its initial distribution at x_0^+ with momentum $\boldsymbol{p}_0$ as

$$\mathcal{W}(\boldsymbol{Y},\boldsymbol{p};x_0^+,x_f^+)=\int \mathrm{d}^2\boldsymbol{X}\mathrm{d}^2\boldsymbol{y}\mathrm{d}^2\boldsymbol{x}\frac{\mathrm{d}^2\boldsymbol{p}_0}{(2\pi)^2}e^{-i\boldsymbol{p}\cdot\boldsymbol{y}+i\boldsymbol{p}_0\cdot\boldsymbol{x}}\mathcal{W}(\boldsymbol{X},\boldsymbol{p}_0;x_0^+,x_0^+)\times\left\langle\!\left\langle U_\parallel\left(\boldsymbol{Y}+\frac{\boldsymbol{y}}{2},x_f^+;\boldsymbol{X}+\frac{\boldsymbol{x}}{2},x_0^+\right)U_\parallel^\dagger\left(\boldsymbol{Y}-\frac{\boldsymbol{y}}{2},x_f^+;\boldsymbol{X}-\frac{\boldsymbol{x}}{2},x_0^+\right)\right\rangle\!\right\rangle, \tag{8}$$

$$\left\langle\!\left\langle U_\parallel\left(\boldsymbol{Y}+\frac{\boldsymbol{y}}{2},x_f^+;\boldsymbol{X}+\frac{\boldsymbol{x}}{2},x_0^+\right)U_\parallel^\dagger\left(\boldsymbol{Y}-\frac{\boldsymbol{y}}{2},x_f^+;\boldsymbol{X}-\frac{\boldsymbol{x}}{2},x_0^+\right)\right\rangle\!\right\rangle=\int_{\boldsymbol{r_1}(x_0^+)=\boldsymbol{X}+\frac{\boldsymbol{x}}{2}}^{\boldsymbol{r_1}(x_f^+)=\boldsymbol{Y}+\frac{\boldsymbol{y}}{2}}\mathcal{D}\boldsymbol{r_1}\int_{\boldsymbol{r_2}(x_0^+)=\boldsymbol{X}-\frac{\boldsymbol{x}}{2}}^{\boldsymbol{r_2}(x_f^+)=\boldsymbol{Y}-\frac{\boldsymbol{y}}{2}}\mathcal{D}\boldsymbol{r_2}\exp\left\{i\frac{p^+}{2}\int_{x_0^+}^{x_f^+}\mathrm{d}t(\dot{\boldsymbol{r}}_1^2-\dot{\boldsymbol{r}}_2^2)\right\}\frac{1}{N_c}\langle\!\langle\mathrm{tr}\{W_\parallel(\boldsymbol{r_1},x_0^+,x_f^+)W_\parallel^\dagger(\boldsymbol{r_2},x_0^+,x_f^+)\}\rangle\!\rangle, \tag{9}$$

where $\langle\!\langle\cdots\rangle\!\rangle$ denotes the average over the proper ensemble of the medium field configurations and $\dot{\boldsymbol{r}}\equiv d\boldsymbol{r}/dx^+$. Note that the trace and the $1/N_c$ factor correspond to the average over the initial color indices in the fundamental representation.

In an arbitrary gauge (either covariant or light-cone gauge), the gauge-invariant quark wave function should be defined as

$$\Psi(\boldsymbol{x},x_0^+,x^+)\equiv\psi(\boldsymbol{x},x^+)W_\parallel(\boldsymbol{x},x_0^+,x^+)W_\perp(\boldsymbol{x},x^+), \tag{10}$$

where the transverse Wilson line is defined as

$$W_\perp(\boldsymbol{x},x^+)\equiv\mathcal{P}\exp\left[ig\int_{\boldsymbol{x}}^{\infty}\mathrm{d}\boldsymbol{\xi}\cdot\boldsymbol{A}_\perp(\boldsymbol{\xi},x^+)\right]. \tag{11}$$

The corresponding evolution operator for the quark propagation is

$$U(\boldsymbol{x}_f,x_f^+;\boldsymbol{x}_0,x_0^+)=\int_{\boldsymbol{r}(x_0^+)=\boldsymbol{x}_0}^{\boldsymbol{r}(x_f^+)=\boldsymbol{x}_f}\mathcal{D}\boldsymbol{r}(x^+)\exp\left[i\frac{p^+}{2}\int\mathrm{d}x^+\left(\frac{d\boldsymbol{r}}{dx^+}\right)^2\right]W(\boldsymbol{r},x_0^+,x_f^+), \tag{12}$$

where $W(\boldsymbol{r},x_0^+,x^+)\equiv W_\parallel(\boldsymbol{r},x_0^+,x^+)W_\perp(\boldsymbol{r},x^+)$. The evolution of the Wigner function should be the same as in the covariant gauge by replacing $W_\parallel(\boldsymbol{r},x_0^+,x^+)$ with $W(\boldsymbol{r},x_0^+,x^+)$ in the evolution operator.

Under the dipole approximation, the expectation value of the correlation of two Wilson lines can be related to the jet transport coefficient $\hat{q}$ [61–63],

$$\frac{1}{N_c}\langle\!\langle\mathrm{tr}\{W(\boldsymbol{r}_1,x_0^+,x_f^+)W^\dagger(\boldsymbol{r}_2,x_0^+,x_f^+)\}\rangle\!\rangle\approx\exp\left\{-\int_{x_0^+}^{x_f^+}\mathrm{d}x^+\frac{1}{4\sqrt{2}}\hat{q}(\boldsymbol{R})\boldsymbol{r}^2\right\}\equiv\exp\left\{-\int_{t_0}^{t_f}\mathrm{d}t\frac{1}{4}\hat{q}(\boldsymbol{R})\boldsymbol{r}^2\right\}, \tag{13}$$

where $\boldsymbol{R}=(\boldsymbol{r}_1+\boldsymbol{r}_2)/2$ and $\boldsymbol{r}=\boldsymbol{r}_1-\boldsymbol{r}_2$. In this expression we are implicitly assuming that the transverse separation $\boldsymbol{r}\sim 1/\boldsymbol{p}$ is much smaller than the scale of variations in $\hat{q}(\boldsymbol{R})$. For convenience, we have redefined the light-cone variables $t=x^+/\sqrt{2}$ and $\omega=p^+/\sqrt{2}$ which become the normal time and energy on the light cone. In a static and homogeneous medium, the correlation will only depend on the relative position of the dipole and the jet transport coefficient will be a constant. Such an approximation is often referred to as the "harmonic approximation." In past studies, the time (x^+ or t)

dependence of $\hat{q}$ was considered. In this study, however, we generalize the dipole approximation to the case in which the jet transport coefficient also has a spatial dependence in the transverse plane. The Wigner distribution of the propagating parton at time t_f is now

$$\mathcal{W}(\boldsymbol{Y},\boldsymbol{p};t_0,t_f)=\int \mathrm{d}^2\boldsymbol{X}\mathrm{d}^2\boldsymbol{y}\mathrm{d}^2\boldsymbol{x}\,\frac{\mathrm{d}^2\boldsymbol{p}_0}{(2\pi)^2}\,e^{-i\boldsymbol{p}\cdot\boldsymbol{y}+i\boldsymbol{p}_0\cdot\boldsymbol{x}}\mathcal{W}(\boldsymbol{X},\boldsymbol{p}_0;t_0,t_0) \times\int_{\boldsymbol{R}(t_0)=\boldsymbol{X}}^{\boldsymbol{R}(t_f)=\boldsymbol{Y}}\mathcal{D}\boldsymbol{R}\int_{\boldsymbol{r}(t_0)=\boldsymbol{x}}^{\boldsymbol{r}(t_f)=\boldsymbol{y}}\mathcal{D}\boldsymbol{r}\exp\left\{i\omega\int_{t_0}^{t_f}\mathrm{d}t\dot{\boldsymbol{R}}\cdot\dot{\boldsymbol{r}}\right\}\exp\left\{-\int_{t_0}^{t_f}\mathrm{d}t\frac{1}{4}\hat{q}(\boldsymbol{R})\boldsymbol{r}^2\right\}. \tag{14}$$

To evaluate the path integral, we discretize the time into N equal steps ($N\to\infty$) and denote $\epsilon=(t_f-t_0)/N$, $t_f=t_N$, and $\boldsymbol{R}(t_k)=\boldsymbol{R}_k$. The second line in Eq. (14) can be expressed as

$$K=\frac{1}{A^{4N}}\left(\prod_{k=1}^{N-1}\int\mathrm{d}^2\boldsymbol{R}_k\right)\exp\left\{i\omega(\dot{\boldsymbol{R}}_N\boldsymbol{r}_N-\dot{\boldsymbol{R}}_0\boldsymbol{r}_0)\right\}\left(\prod_{k=1}^{N-1}\int\mathrm{d}^2\boldsymbol{r}_k\exp\left\{-\epsilon\frac{\hat{q}(\boldsymbol{R}_k)}{4}\left(\boldsymbol{r}_k^2+\frac{4i\omega}{\hat{q}(\boldsymbol{R}_k)}\ddot{\boldsymbol{R}}_k\boldsymbol{r}_k\right)\right\}\right), \tag{15}$$

where $A=\sqrt{2\pi i\epsilon/\omega}$. More details on the evaluation of the functional measure can be found in Appendix A. Completing the squares and performing a Gaussian functional integral to integrate over the relative distance $\boldsymbol{r}$, and switching back to the continuous form, Eq. (14) can be rewritten as

$$\mathcal{W}(\boldsymbol{Y},\boldsymbol{p};t_0,t_f)=\int \mathrm{d}^2\boldsymbol{X}\mathrm{d}^2\boldsymbol{y}\mathrm{d}^2\boldsymbol{x}\,\frac{d^2\boldsymbol{p}_0}{(2\pi)^2}\,e^{-i\boldsymbol{p}\cdot\boldsymbol{y}+i\boldsymbol{p}_0\cdot\boldsymbol{x}}\mathcal{W}(\boldsymbol{X},\boldsymbol{p}_0;t_0,t_0) \times\mathcal{Z}\int_{\boldsymbol{R}(t_0)=\boldsymbol{X}}^{\boldsymbol{R}(t_f)=\boldsymbol{Y}}\mathcal{D}\boldsymbol{R}\exp\{i\omega(\dot{\boldsymbol{R}}(t_f)\boldsymbol{y}-\dot{\boldsymbol{R}}(t_0)\boldsymbol{x})\}\exp\left\{-\int_{t_0}^{t_f}\mathrm{d}t\frac{\omega^2\ddot{\boldsymbol{R}}^2}{\hat{q}(\boldsymbol{R})}\right\}, \tag{16}$$

where

$$\mathcal{Z}=\frac{2^{3N}\omega^N}{4\pi\epsilon^{2N-1}}\frac{1}{\det\{\hat{q}(\boldsymbol{R})\}} \tag{17}$$

is a divergent normalization constant and

$$\frac{1}{\det\{\hat{q}(\boldsymbol{R})\}}=\prod_{k=1}^{N-1}\frac{1}{\hat{q}(\boldsymbol{R}_k)}. \tag{18}$$

Note that in the above expression, the initial and final transverse momenta are given by the classical momenta of a particle with mass ω which follows a trajectory $\boldsymbol{R}(t)$.

To proceed, we introduce a two-dimensional auxiliary variable $\boldsymbol{\xi}=(\xi^a,\xi^b)$ by defining

$$\boldsymbol{\xi}=\omega\ddot{\boldsymbol{R}}\quad\text{or}\quad 1=\mathcal{A}\int\mathcal{D}\boldsymbol{\xi}\delta(\boldsymbol{\xi}-\omega\ddot{\boldsymbol{R}}), \tag{19}$$

where $\mathcal{A}$ is a normalization constant and $\delta(\boldsymbol{\xi}-\omega\ddot{\boldsymbol{R}})$ is a functional delta function. We note that $\boldsymbol{\xi}$ as so defined can be interpreted as a random force acting on the hard particle with effective mass ω.

Again, after discretizing the space-time, we can write down the expression for $\boldsymbol{\xi}$ at t_k as

$$\boldsymbol{\xi}_k=\omega\ddot{\boldsymbol{R}}_k=\omega\frac{\boldsymbol{R}_{k+1}-2\boldsymbol{R}_k+\boldsymbol{R}_{k-1}}{\epsilon^2}. \tag{20}$$

Replacing the variable $\boldsymbol{R}$ with $\boldsymbol{\xi}$ and using the Jacobian of the transformation,

$$J\equiv\frac{(\partial\xi_1^a\cdots\partial\xi_{N-1}^a)}{(\partial R_1^a\cdots\partial R_{N-1}^a)}=\left(\frac{-2\omega}{\epsilon^2}\right)^{N-1}\times\det\begin{pmatrix}1&-\frac{1}{2}&0&0&\ldots&0\\-\frac{1}{2}&1&-\frac{1}{2}&0&\ldots&0\\0&-\frac{1}{2}&1&-\frac{1}{2}&\ldots&0\\\vdots&\vdots&\ddots&\ddots&\ddots&\vdots\\0&\ldots&0&-\frac{1}{2}&1&-\frac{1}{2}\\0&\ldots&0&0&-\frac{1}{2}&1\end{pmatrix}_{(N-1)\times(N-1)}=N\left(\frac{\omega}{\epsilon^2}\right)^{N-1}, \tag{21}$$

we can rewrite Eq. (15) in terms of a functional integral with respect to $\boldsymbol{\xi}$,

$$K = \frac{1}{4\pi^2}\left(\frac{\omega}{t_f - t_0}\right)^2 \int \widehat{\mathcal{D}}\boldsymbol{\xi} \exp\{i\omega(\dot{\boldsymbol{R}}(t_f)\boldsymbol{y} - \dot{\boldsymbol{R}}(t_0)\boldsymbol{x})\} \exp\left\{-\int_{t_0}^{t_f} \mathrm{d}t \frac{\boldsymbol{\xi}(t)^2}{\hat{q}(\boldsymbol{R})}\right\}, \tag{22}$$

and the Wigner function in Eq. (16) as

$$\mathcal{W}(\boldsymbol{Y},\boldsymbol{p};t_0,t_f) = \left(\frac{\omega}{t_f - t_0}\right)^2 \int \mathrm{d}^2\boldsymbol{X}\mathrm{d}^2\boldsymbol{p}_0 \mathcal{W}(\boldsymbol{X},\boldsymbol{p}_0;t_0,t_0) \times \int \widehat{\mathcal{D}}\boldsymbol{\xi}\delta^2(\omega\dot{\boldsymbol{R}}(t_0,\boldsymbol{\xi}) - \boldsymbol{p}_0)\delta^2(\omega\dot{\boldsymbol{R}}(t_f,\boldsymbol{\xi}) - \boldsymbol{p}) \exp\left\{-\int_{t_0}^{t_f} \mathrm{d}t \frac{\boldsymbol{\xi}(t)^2}{\hat{q}(\boldsymbol{R})}\right\}, \tag{23}$$

where we have defined

$$\hat{\mathcal{D}}\boldsymbol{\xi} = \frac{1}{\det\{\hat{q}(\boldsymbol{R})\}} \prod_{k=1}^{N-1}\left(\frac{\epsilon}{\pi}\right) d^2\boldsymbol{\xi}_k, \tag{24}$$

such that

$$\int \widehat{\mathcal{D}}\boldsymbol{\xi} \exp\left\{-\int \mathrm{d}t \frac{\boldsymbol{\xi}(t)^2}{\hat{q}(\boldsymbol{R})}\right\} = 1. \tag{25}$$

See Appendix B for more details on this. With such a normalization condition above, we can interpret the functional integrand

$$\frac{1}{\det\{\hat{q}(\boldsymbol{R})\}} \exp\left\{-\int \mathrm{d}t \frac{\boldsymbol{\xi}(t)^2}{\hat{q}(\boldsymbol{R})}\right\} \tag{26}$$

as a Gaussian probability distribution of the random force $\boldsymbol{\xi}$, driving the Brownian-motion-like transverse momentum broadening of the propagating parton in the QGP medium.

With this probability distribution, averaging for any function $f(\boldsymbol{\xi})$ over the random variable $\boldsymbol{\xi}$ can now be computed as a functional integral,

$$\langle f(\boldsymbol{\xi})\rangle = \int \widehat{\mathcal{D}}\boldsymbol{\xi} f(\boldsymbol{\xi}) \exp\left\{-\int \mathrm{d}t \frac{\boldsymbol{\xi}(t)^2}{\hat{q}(\boldsymbol{R})}\right\}. \tag{27}$$

For parton propagation in a uniform medium with a constant jet transport coefficient $\hat{q}(\boldsymbol{R}) = \hat{q}_0$, the two-point correlation function is (see Appendix C for details)

$$\langle \xi^i(t)\xi^j(t')\rangle_0 = \int \widehat{\mathcal{D}}\boldsymbol{\xi}\{\xi^i(t)\xi^j(t')\} \exp\left\{-\int \mathrm{d}t \frac{\boldsymbol{\xi}^2}{\hat{q}_0}\right\} = \frac{\hat{q}_0}{2}\delta^{ij}\delta(t - t'). \tag{28}$$

As we noted before, $\boldsymbol{\xi}$ can be considered as a random force acting on a particle with an effective mass ω on a classical trajectory. The boundary conditions for the trajectory are

$$\boldsymbol{R}(t_0,\boldsymbol{\xi}) = \boldsymbol{X}, \qquad \boldsymbol{R}(t_f,\boldsymbol{\xi}) = \boldsymbol{Y} \tag{29}$$

at the initial time t_0 and the final time t_f, respectively, during which the random force $\boldsymbol{\xi}$ gives rise to a displacement

$$\boldsymbol{Y} - \boldsymbol{X} = (t_f - t_0)\dot{\boldsymbol{R}}(t_0,\boldsymbol{\xi}) + \int_{t_0}^{t_f} \mathrm{d}t' \int_{t_0}^{t'} \mathrm{d}t'' \frac{\boldsymbol{\xi}(t'')}{\omega}. \tag{30}$$

The initial velocity of the particle is therefore

$$\dot{\boldsymbol{R}}(t_0,\boldsymbol{\xi}) = \frac{\boldsymbol{p}_0}{\omega} = \frac{1}{t_f - t_0}\left(\boldsymbol{Y} - \boldsymbol{X} - \int_{t_0}^{t_f} \mathrm{d}t' \int_{t_0}^{t'} \mathrm{d}t'' \frac{\boldsymbol{\xi}(t'')}{\omega}\right). \tag{31}$$

The velocity of the particle at any given time t should be

$$\dot{\boldsymbol{R}}(t,\boldsymbol{\xi}) = \dot{\boldsymbol{R}}(t_0,\boldsymbol{\xi}) + \int_{t_0}^{t} \mathrm{d}t'' \frac{\boldsymbol{\xi}(t'')}{\omega}, \tag{32}$$

and the position of this particle is given by

$$\boldsymbol{R}(t,\boldsymbol{\xi}) = \boldsymbol{X} + (t - t_0)\frac{\boldsymbol{p}_0}{\omega} + \frac{1}{\omega}\int_{t_0}^{t} \mathrm{d}t'(t - t')\boldsymbol{\xi}(t'). \tag{33}$$

In arriving at the last equation for the position $\boldsymbol{R}(t,\boldsymbol{\xi})$, the following identity is used for an arbitrary smooth function $f(t)$:

$$\int_{t_0}^{t} \mathrm{d}t' \int_{t_0}^{t'} \mathrm{d}t'' f(t'') = \int_{t_0}^{t} \mathrm{d}t'(t - t')f(t'). \tag{34}$$

Substituting the particle velocities in Eqs. (31) and (32) into the delta function in the Wigner function in Eq. (23), we arrive at

$$\mathcal{W}(\boldsymbol{Y},\boldsymbol{p};t_0,t_f)=\left(\frac{\omega}{t_f-t_0}\right)^2\int \mathrm{d}^2\boldsymbol{X}\mathrm{d}^2\boldsymbol{p}_0\mathcal{W}(\boldsymbol{X},\boldsymbol{p}_0;t_0,t_0)\int\frac{\mathrm{d}^2\boldsymbol{x}}{(2\pi)^2}\frac{\mathrm{d}^2\boldsymbol{y}}{(2\pi)^2}\exp\left\{i\frac{\omega(\boldsymbol{Y}-\boldsymbol{X})}{t_f-t_0}\cdot(\boldsymbol{y}-\boldsymbol{x})+i\boldsymbol{p}_0\cdot\boldsymbol{x}-i\boldsymbol{p}\cdot\boldsymbol{y}\right\}$$
$$\times\int\widehat{\mathcal{D}}\boldsymbol{\xi}\exp\left\{-\int_{t_0}^{t_f}\mathrm{d}t\frac{\boldsymbol{\xi}(t)^2}{\hat{q}(\boldsymbol{R})}\right\}\exp\left\{i(\boldsymbol{x}-\boldsymbol{y})\cdot\int_{t_0}^{t_f}\mathrm{d}t'\int_{t_0}^{t'}\mathrm{d}t''\frac{\boldsymbol{\xi}(t'')}{t_f-t_0}+i\boldsymbol{y}\cdot\int_{t_0}^{t_f}\mathrm{d}t\boldsymbol{\xi}(t)\right\}. \tag{35}$$

Performing the integration over $\boldsymbol{p}$ or $\boldsymbol{Y}$, we can get the transverse position or transverse momentum distribution of the propagating parton at time t_f, respectively,

$$\frac{d^2N}{d^2\boldsymbol{Y}}=\left(\frac{\omega}{t_f-t_0}\right)^2\int \mathrm{d}^2\boldsymbol{X}\mathrm{d}^2\boldsymbol{p}_0\frac{\mathrm{d}^2\boldsymbol{x}}{(2\pi)^2}\mathcal{W}(\boldsymbol{X},\boldsymbol{p}_0;t_0,t_0)e^{-i\boldsymbol{x}\cdot(\frac{\omega(\boldsymbol{Y}-\boldsymbol{X})}{t_f-t_0}-\boldsymbol{p}_0)}\int\widehat{\mathcal{D}}\boldsymbol{\xi}\exp\left\{i\boldsymbol{x}\cdot\int_{t_0}^{t_f}\mathrm{d}t'\int_{t_0}^{t'}\mathrm{d}t''\frac{\boldsymbol{\xi}(t'')}{t_f-t_0}-\int_{t_0}^{t_f}\mathrm{d}t\frac{\boldsymbol{\xi}(t)^2}{\hat{q}(\boldsymbol{R})}\right\}, \tag{36}$$

$$\frac{d^2N}{d^2\boldsymbol{p}}=\int \mathrm{d}^2\boldsymbol{X}\mathrm{d}^2\boldsymbol{p}_0\frac{\mathrm{d}^2\boldsymbol{x}}{(2\pi)^2}\mathcal{W}(\boldsymbol{X},\boldsymbol{p}_0;t_0,t_0)e^{-i\boldsymbol{x}\cdot(\boldsymbol{p}-\boldsymbol{p}_0)}\int\widehat{\mathcal{D}}\boldsymbol{\xi}\exp\left\{i\boldsymbol{x}\cdot\int_{t_0}^{t_f}\mathrm{d}t\boldsymbol{\xi}(t)-\int_{t_0}^{t_f}\mathrm{d}t\frac{\boldsymbol{\xi}(t)^2}{\hat{q}(\boldsymbol{R})}\right\}. \tag{37}$$

III. SPECTRA IN UNIFORM MEDIUM

The general expression for the final phase-space distribution of a propagating parton in terms of path integrals is valid for a dynamic and inhomogeneous medium in the transverse plane. In the special case of a static and uniform QGP medium in which the jet transport coefficient is a constant $\hat{q}(\boldsymbol{R})=\hat{q}_0$, one can complete the path integral in Eqs. (35)–(37). The distributions can be greatly simplified as (more details on the derivation are given in Appendix D)

$$\mathcal{W}_0(\boldsymbol{Y},\boldsymbol{p};t_0,t_f)=\frac{12\omega^2}{\pi^2\hat{q}_0^2(t_f-t_0)^4}\int \mathrm{d}^2\boldsymbol{X}\mathrm{d}^2\boldsymbol{p}_0\mathcal{W}(\boldsymbol{X},\boldsymbol{p}_0;t_0,t_0)$$
$$\times\exp\left\{\frac{-12\omega^2}{\hat{q}_0(t_f-t_0)^3}\left((\boldsymbol{Y}-\boldsymbol{X})-\frac{t_f-t_0}{2\omega}(\boldsymbol{p}+\boldsymbol{p}_0)\right)^2-\frac{(\boldsymbol{p}-\boldsymbol{p}_0)^2}{\hat{q}_0(t_f-t_0)}\right\}, \tag{38}$$

$$\frac{d^2N_0}{d^2\boldsymbol{p}}=\frac{1}{\pi\hat{q}_0(t_f-t_0)}\int \mathrm{d}^2\boldsymbol{X}\mathrm{d}^2\boldsymbol{p}_0\mathcal{W}(\boldsymbol{X},\boldsymbol{p}_0;t_0,t_0)\exp\left\{-\frac{(\boldsymbol{p}-\boldsymbol{p}_0)^2}{\hat{q}_0(t_f-t_0)}\right\}, \tag{39}$$

$$\frac{d^2N_0}{d^2\boldsymbol{Y}}=\frac{3\omega^2}{\pi\hat{q}_0(t_f-t_0)^3}\int \mathrm{d}^2\boldsymbol{X}\mathrm{d}^2\boldsymbol{p}_0\mathcal{W}(\boldsymbol{X},\boldsymbol{p}_0;t_0,t_0)\exp\left\{-\frac{3(\omega\frac{\boldsymbol{Y}-\boldsymbol{X}}{t_f-t_0}-\boldsymbol{p}_0)^2}{\hat{q}_0(t_f-t_0)}\right\} \tag{40}$$

for any given initial Wigner distribution $\mathcal{W}(\boldsymbol{X},\boldsymbol{p}_0;t_0,t_0)$.

For an initial point-like classical particle with specific initial momentum and position $\mathcal{W}(\boldsymbol{X},\boldsymbol{p}_0;t_0,t_0)=(2\pi)^2\delta^2(\boldsymbol{X})\delta^2(\boldsymbol{p}_0)$, the final Wigner function at a later time t_f becomes

$$\mathcal{W}_0(\boldsymbol{Y},\boldsymbol{p};t_0,t_f)=3\frac{(4\omega)^2}{\hat{q}_0^2(t_f-t_0)^4}\exp\left\{\frac{-12\omega^2}{\hat{q}_0(t_f-t_0)^3}\left(\boldsymbol{Y}-\frac{t_f-t_0}{2\omega}\boldsymbol{p}\right)^2-\frac{\boldsymbol{p}^2}{\hat{q}_0(t_f-t_0)}\right\}$$
$$=3\frac{(4\omega)^2}{\hat{q}_0^2(t_f-t_0)^4}\exp\left\{-\left(\boldsymbol{p}-\frac{3\omega}{2(t_f-t_0)}\boldsymbol{Y}\right)^2\frac{4}{\hat{q}_0(t_f-t_0)}-\boldsymbol{Y}^2\frac{3\omega^2}{\hat{q}_0(t_f-t_0)^3}\right\}. \tag{41}$$

One can verify that the final Wigner distribution functions in Eqs. (38) and (41) satisfy the drift-diffusion equation,

$$\left(\frac{\partial}{\partial t}+\frac{\boldsymbol{p}}{\omega}\cdot\boldsymbol{\nabla}_{\boldsymbol{Y}}\right)\mathcal{W}_0(\boldsymbol{Y},\boldsymbol{p};t_0,t)=\frac{\hat{q}_0}{4}\boldsymbol{\nabla}_{\boldsymbol{p}}^2\mathcal{W}_0(\boldsymbol{Y},\boldsymbol{p};t_0,t), \tag{42}$$

which is just the Boltzmann equation under the special approximation of small-angle scattering whose solution for an initial classical point-like particle in a uniform medium as shown in Eq. (41) was first obtained in Ref. [49]. Indeed, as shown in Fig. 3, apart from the usual diffusion in both transverse momentum and coordinate, the Wigner distribution develops a drift $\frac{t_f-t_0}{2\omega}\boldsymbol{p}$ in the transverse coordinate for a given value of the transverse momentum $\boldsymbol{p}$ and a drift $\frac{3\omega}{2(t_f-t_0)}\boldsymbol{Y}$ in the transverse momentum for a given value of

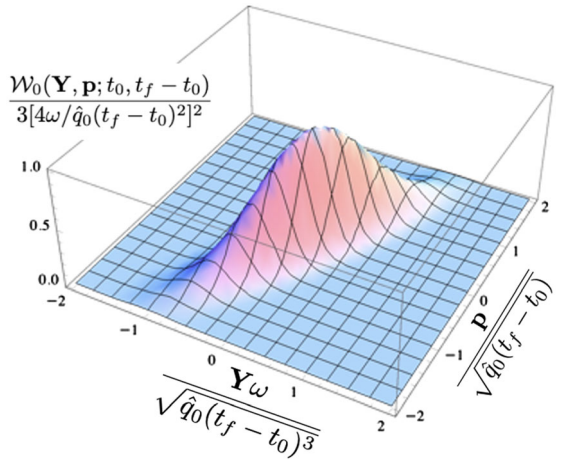

FIG. 3. Scaled Wigner distribution for an initial classical parton in a uniform medium with a constant jet transport coefficient $\hat{q}_0$ given by Eq. (41) as a function of the transverse momentum and coordinate, both scaled by their respective widths $\sqrt{\hat{q}_0(t_f-t_0)}$ and $\sqrt{\hat{q}_0(t_f-t_0)^3}/\omega$.

the transverse coordinate $\boldsymbol{Y}$. The Gaussian diffusion width in the transverse momentum $\sqrt{\hat{q}_0(t_f-t_0)}$ is the typical momentum broadening during the given time interval. The diffusion width in the transverse position is given by the average transverse velocity $\sqrt{\hat{q}_0(t_f-t_0)}/\omega$ times the time interval or $\sqrt{\hat{q}_0(t_f-t_0)^3}/\omega$.

Integrating over the transverse coordinate $\mathbf{Y}$ or the transverse momentum $\mathbf{p}$, the Wigner distribution in Eq. (41) gives the diffusion distributions in the transverse momentum and transverse coordinate, respectively,

$$\frac{d^2N}{d^2\boldsymbol{p}}=\frac{(2\pi)^2}{\pi\hat{q}_0(t_f-t_0)}\exp\left\{-\frac{\boldsymbol{p}^2}{\hat{q}_0(t_f-t_0)}\right\}, \tag{43}$$

$$\frac{d^2N}{d^2\boldsymbol{Y}}=\frac{(2\pi)^2 3\omega^2}{\pi\hat{q}_0(t_f-t_0)^3}\exp\left\{-\frac{3(\omega\boldsymbol{Y})^2}{\hat{q}_0(t_f-t_0)^3}\right\}, \tag{44}$$

which satisfy the usual Fokker-Planck diffusion equation. We note that the diffusion distribution in the transverse momentum has been obtained within the framework of the higher-twist formalism under the maximal two-gluon correlation approximation [63] and by a direct summation of multiple scatterings [64].

IV. TRANSVERSE MOMENTUM ASYMMETRY IN NONUNIFORM MEDIUM

To investigate the momentum diffusion in a nonuniform medium within the path-integral approach, we consider a simple transverse distribution of the jet transport coefficient,

$$\hat{q}(\boldsymbol{R})=\frac{\hat{q}_0}{1-f(\boldsymbol{R})}, \tag{45}$$

with $f(\boldsymbol{R})\ll 1$ for all values of $\boldsymbol{R}$. This corresponds to a static medium that is uniform in the direction of the parton propagation but varies in the transverse direction. We should emphasize that this simple setup allows us to complete the path integral analytically but it is far from the realistic case in high-energy heavy-ion collisions where the medium is nonuniform in both the transverse and longitudinal directions of parton propagation.

For convenience we denote the functional integral part in Eq. (37) for the final momentum spectrum as

$$F(\boldsymbol{x},\boldsymbol{X},\boldsymbol{p}_0)=\int\widehat{\mathcal{D}}\boldsymbol{\xi}\exp\left\{\int_{t_0}^{t_f}\mathrm{d}t\left[i\boldsymbol{x}\cdot\boldsymbol{\xi}(t)-\frac{\boldsymbol{\xi}(t)^2}{\hat{q}(\boldsymbol{R})}\right]\right\}. \tag{46}$$

With the variable transformation $\boldsymbol{\xi}'=\boldsymbol{\xi}-i\frac{\hat{q}_0}{2}\boldsymbol{x}$ and to the leading order in f, it can be approximately rewritten as (see Appendix E for more details)

$$F(\boldsymbol{x},\boldsymbol{X},\boldsymbol{p}_0)\approx\exp\left\{-\int_{t_0}^{t_f}\mathrm{d}t\frac{\hat{q}_0}{4}\boldsymbol{x}^2\right\}\times\left[1-\boldsymbol{x}^2\int_{t_0}^{t_f}\mathrm{d}t\frac{\hat{q}_0}{4}\langle f(\boldsymbol{R}(t,\boldsymbol{\xi}'(t)))\rangle_0\right], \tag{47}$$

where the average $\langle\cdots\rangle_0$ is defined as

$$\langle\cdots\rangle_0\equiv\int\widehat{\mathcal{D}}\boldsymbol{\xi}'(\cdots)\exp\left\{-\int\mathrm{d}t\frac{(\boldsymbol{\xi}'(t))^2}{\hat{q}_0}\right\}. \tag{48}$$

The classical trajectory of the particle presented in Eq. (33) can be rewritten as

$$\boldsymbol{R}(t,\boldsymbol{\xi}')\equiv\boldsymbol{R}_0(t)+\Delta\boldsymbol{R}(t,\boldsymbol{\xi}'), \tag{49}$$

with

$$\begin{aligned}\boldsymbol{R}_0(t)&\equiv\boldsymbol{X}+(t-t_0)\frac{\boldsymbol{p}_0}{\omega}+i\boldsymbol{x}\frac{\hat{q}_0}{4\omega}(t-t_0)^2,\\ \Delta\boldsymbol{R}(t,\boldsymbol{\xi}')&\equiv\frac{1}{\omega}\int_{t_0}^{t}\mathrm{d}t'(t-t')\boldsymbol{\xi}'(t').\end{aligned} \tag{50}$$

Since only $\Delta\boldsymbol{R}(t,\boldsymbol{\xi}')$ contains the effect of the noise $\boldsymbol{\xi}'$, we can treat it as a perturbation and expand $f(\boldsymbol{R})$ perturbatively,

$$f(\boldsymbol{R}(t,\boldsymbol{\xi}'))=\sum_{n=0}^{\infty}\frac{1}{n!}\sum_{i_1,\ldots,i_n=1}^{2}\Delta R^{i_1}(t,\boldsymbol{\xi}')\cdots\Delta R^{i_n}(t,\boldsymbol{\xi}')\times(\nabla_{i_1}\nabla_{i_2}\cdots\nabla_{i_n}f(\boldsymbol{R}(t,\boldsymbol{\xi}')))_{\boldsymbol{R}(t,\boldsymbol{\xi}')=\boldsymbol{R}_0(t)}, \tag{51}$$

where $\nabla_i = \frac{\partial}{\partial R_i}$. Using the correlators

$$\langle \Delta R^i(t,\boldsymbol{\xi}')\rangle_0 = 0, \tag{52}$$

$$\langle \Delta R^i(t,\boldsymbol{\xi}')\Delta R^j(t,\boldsymbol{\xi}')\rangle_0 = \frac{1}{\omega^2}\frac{\hat{q}_0}{2}\delta^{ij}\frac{(t-t_0)^3}{3}, \tag{53}$$

$$\langle \Delta R^{i_1}(t,\boldsymbol{\xi}')\Delta R^{i_2}(t,\boldsymbol{\xi}')\cdots\Delta R^{i_{2n-1}}(t,\boldsymbol{\xi}')\rangle_0 = 0, \tag{54}$$

$$\begin{aligned}&\langle \Delta R^{i_1}\Delta R^{i_2}\cdots\Delta R^{i_{2n}}(t,\boldsymbol{\xi}')\rangle_0 \\ &= \langle \Delta R^{i_1}\Delta R^{i_2}(t,\boldsymbol{\xi}')\rangle_0\cdots\langle \Delta R^{i_{2n-1}}\Delta R^{i_{2n}}(t,\boldsymbol{\xi}')\rangle_0 \\ &\quad + \text{all other permutations},\end{aligned} \tag{55}$$

where the total number of permutations is $(2n-1)!!$, we can substitute the expansion of $f(\boldsymbol{R})$ in Eq. (51) into Eq. (47) and obtain

$$\begin{aligned}F(\boldsymbol{x},\boldsymbol{X},\boldsymbol{p}_0) &= \exp\left\{-\int_{t_0}^{t_f}\mathrm{d}t\frac{\hat{q}_0}{4}\boldsymbol{x}^2\right\}\left[1-\boldsymbol{x}^2\int_{t_0}^{t_f}\mathrm{d}t\frac{\hat{q}_0}{4}\sum_{n=0}^{\infty}\frac{2^n(2n-1)!!}{(2n)!}\left(\frac{\hat{q}_0(t-t_0)^3}{12\omega^2}\right)^n((\boldsymbol{\nabla}_{\boldsymbol{R}}^2)^n f(\boldsymbol{R}(t,\boldsymbol{\xi}')))_{\boldsymbol{R}(t,\boldsymbol{\xi}')=\boldsymbol{R}_0(t)}\right] \\ &= \exp\left\{-\int_{t_0}^{t_f}\mathrm{d}t\frac{\hat{q}_0}{4}\boldsymbol{x}^2\right\}\left[1-\boldsymbol{x}^2\int_{t_0}^{t_f}\mathrm{d}t\frac{\hat{q}_0}{4}\Phi(\boldsymbol{R}_0(t))\right],\end{aligned} \tag{56}$$

where

$$\begin{aligned}\Phi(\boldsymbol{R}(t)) &= \sum_{n=0}^{\infty}\frac{(D(t-t_0)^3\boldsymbol{\nabla}_{\boldsymbol{R}}^2)^n}{n!}f(\boldsymbol{R}(t)), \\ &= \int \mathrm{d}^2\tilde{\boldsymbol{R}}\frac{f(\tilde{\boldsymbol{R}})}{4\pi D(t-t_0)^3}\exp\left[-\frac{(\boldsymbol{R}(t)-\tilde{\boldsymbol{R}})^2}{4D(t-t_0)^3}\right],\end{aligned} \tag{57}$$

$$\Phi(\boldsymbol{R}_0(t)) = \Phi(\boldsymbol{R}(t))|_{\boldsymbol{R}(t)=\boldsymbol{R}_0(t)}, \tag{58}$$

and $D \equiv \hat{q}_0/12\omega^2$.

With the above approximation of the path integral, we can obtain the transverse momentum distribution,

$$\frac{d^2N}{d^2\boldsymbol{p}} \approx \frac{d^2N_0}{d^2\boldsymbol{p}} + \frac{d^2N_1}{d^2\boldsymbol{p}}, \tag{59}$$

with $d^2N_0/d^2\boldsymbol{p}$ given by the solution for a parton propagating in a uniform medium in Eq. (39), and

$$\frac{d^2N_1}{d^2\boldsymbol{p}} = -\int \mathrm{d}^2\boldsymbol{X}\mathrm{d}^2\boldsymbol{p}_0\frac{\mathrm{d}^2\boldsymbol{x}}{(2\pi)^2}\mathcal{W}(\boldsymbol{X},\boldsymbol{p}_0;t_0,t_0)e^{-i\boldsymbol{x}\cdot(\boldsymbol{p}-\boldsymbol{p}_0)}\exp\left\{-\int_{t_0}^{t_f}\mathrm{d}t\frac{\hat{q}_0}{4}\boldsymbol{x}^2\right\}\left[\boldsymbol{x}^2\int_{t_0}^{t_f}\mathrm{d}t\frac{\hat{q}_0}{4}\Phi(\boldsymbol{R}_0(t))\right] \tag{60}$$

is the correction linear in $f(\boldsymbol{R})$ due to the inhomogeneity of the medium. This linear correction can be rewritten as

$$\frac{d^2N_1}{d^2\boldsymbol{p}} = -\int_{t_0}^{t_f}\mathrm{d}t\frac{\hat{q}_0}{4}\int \mathrm{d}^2\boldsymbol{X}\mathrm{d}^2\boldsymbol{p}_0\mathcal{W}(\boldsymbol{X},\boldsymbol{p}_0;t_0,t_0)G(\boldsymbol{p},\boldsymbol{p}_0;\boldsymbol{X},t_f,t,t_0), \tag{61}$$

where the evolution function is defined as

$$G(\boldsymbol{p},\boldsymbol{p}_0;\boldsymbol{X},t_f,t,t_0) = \int\frac{\mathrm{d}^2\boldsymbol{x}}{(2\pi)^2}e^{-i\boldsymbol{x}\cdot(\boldsymbol{p}-\boldsymbol{p}_0)}\exp\left\{-\int_{t_0}^{t_f}\mathrm{d}t\frac{\hat{q}_0}{4}\boldsymbol{x}^2\right\}[\boldsymbol{x}^2\Phi(\boldsymbol{R}_0(t))]. \tag{62}$$

For a Gaussian form of $f(\boldsymbol{R})$,

$$f(\boldsymbol{R}) = \delta\exp\left\{\frac{-\boldsymbol{R}^2}{\sigma^2}\right\}, \tag{63}$$

the jet transport coefficient in Eq. (45) describes a medium that has an increased density within a radius of σ in a uniform medium. One can complete the integration in Eq. (57) and obtain

$$\Phi(\boldsymbol{R}(t)) = \frac{\sigma^2\delta}{\Sigma(t)}\exp\left\{\frac{-\boldsymbol{R}(t)^2}{\Sigma(t)}\right\}, \tag{64}$$

where

$$\Sigma(t) \equiv \sigma^2 + 4D(t-t_0)^3 = \sigma^2 + \frac{\hat{q}_0(t-t_0)^3}{3\omega^2}. \tag{65}$$

The evolution function in Eq. (62) becomes

$$\begin{aligned} G(\boldsymbol{p},\boldsymbol{p}_0;\boldsymbol{X},t_f,t,t_0) &= \int \frac{\mathrm{d}^2\boldsymbol{x}}{(2\pi)^2} e^{-i\boldsymbol{x}\cdot(\boldsymbol{p}-\boldsymbol{p}_0)} \exp\left\{-\frac{\hat{q}_0(t_f-t_0)}{4}\boldsymbol{x}^2\right\}\left[\boldsymbol{x}^2\frac{\sigma^2\delta}{\Sigma(t)}\exp\left\{\frac{-[\boldsymbol{X}+(t-t_0)\frac{\boldsymbol{p}_0}{\omega}+i\boldsymbol{x}\frac{\hat{q}_0}{4\omega}(t-t_0)^2]^2}{\Sigma(t)}\right\}\right] \\ &= \frac{1}{(2\pi)^2}\frac{-16\pi\sigma^2\delta}{\Sigma(t)\Delta^3(t)}\exp\left\{\frac{-(\boldsymbol{X}+(t-t_0)\frac{\boldsymbol{p}_0}{\omega})^2}{\Sigma(t)}\right\}\exp\left\{-\frac{[\boldsymbol{p}-\boldsymbol{p}_0+\lambda(t)(\boldsymbol{X}+(t-t_0)\frac{\boldsymbol{p}_0}{\omega})]^2}{\Delta(t)}\right\} \\ &\quad\times\left\{\left[\boldsymbol{p}-\boldsymbol{p}_0+\lambda(t)\left(\boldsymbol{X}+(t-t_0)\frac{\boldsymbol{p}_0}{\omega}\right)\right]-\Delta(t)\right\}, \end{aligned} \tag{66}$$

where

$$\begin{aligned} \Delta(t) &\equiv \hat{q}_0(t_f-t_0)\left(1-\frac{3}{4}\frac{t-t_0}{t_f-t_0}\frac{4D(t-t_0)^3}{\Sigma(t)}\right) \\ &= \hat{q}_0(t_f-t_0)\left(1-\frac{3}{4}\frac{t-t_0}{t_f-t_0}\frac{\hat{q}_0(t-t_0)^3}{3\omega^2\Sigma(t)}\right), \end{aligned} \tag{67}$$

$$\lambda(t) \equiv \frac{\hat{q}_0(t-t_0)^2}{2\omega\Sigma(t)}. \tag{68}$$

For a parton with initial transverse momentum $\boldsymbol{p}_0$ produced at $\mathbf{x} \equiv (x,y)$, the corresponding initial Wigner function is

$$\mathcal{W}(\boldsymbol{X},\boldsymbol{p};t_0,t_0) = (2\pi)^2\delta^2(\mathbf{p}-\mathbf{p}_0)\delta^2(\mathbf{X}-\mathbf{x}). \tag{69}$$

The final transverse momentum distribution at time t_f in Eq. (59) is now

$$\frac{d^2N_0}{d^2\boldsymbol{p}} = \frac{4\pi}{\hat{q}_0(t_f-t_0)}\exp\left\{-\frac{(\boldsymbol{p}-\boldsymbol{p}_0)^2}{\hat{q}_0(t_f-t_0)}\right\}, \tag{70}$$

$$\begin{aligned} \frac{d^2N_1}{d^2\boldsymbol{p}} &= \int_{t_0}^{t_f}\mathrm{d}t\frac{4\pi\hat{q}_0\sigma^2\delta}{\Sigma(t)\Delta(t)}\exp\left\{-\frac{(\mathbf{x}+(t-t_0)\frac{\boldsymbol{p}_0}{\omega})^2}{\Sigma(t)}-\frac{[\boldsymbol{p}-\boldsymbol{p}_0+\lambda(t)(\mathbf{x}+(t-t_0)\frac{\boldsymbol{p}_0}{\omega})]^2}{\Delta(t)}\right\} \\ &\quad\times\frac{1}{\Delta^2(t)}\left\{\left[\boldsymbol{p}-\boldsymbol{p}_0+\lambda(t)\left(\mathbf{x}+(t-t_0)\frac{\boldsymbol{p}_0}{\omega}\right)\right]^2-\Delta(t)\right\}. \end{aligned} \tag{71}$$

For a parton with initial transverse momentum $\mathbf{p}_0 = 0$, the above final distributions become

$$\frac{d^2N_0}{d^2\boldsymbol{p}} = \frac{4\pi}{\hat{q}_0(t_f-t_0)}\exp\left\{-\frac{\boldsymbol{p}^2}{\hat{q}_0(t_f-t_0)}\right\}, \tag{72}$$

$$\begin{aligned} \frac{d^2N_1}{d^2\boldsymbol{p}} &= \int_{t_0}^{t_f}\mathrm{d}t\frac{4\pi\hat{q}_0\sigma^2\delta}{\Sigma(t)\Delta^3(t)}\exp\left\{-\frac{\mathbf{x}^2}{\Sigma(t)}-\frac{[\boldsymbol{p}+\lambda(t)\mathbf{x}]^2}{\Delta(t)}\right\} \\ &\quad\times\{[\boldsymbol{p}+\lambda(t)\mathbf{x}]^2-\Delta(t)\}. \end{aligned} \tag{73}$$

Since $d^2N_0/d^2\mathbf{p}$ is the solution to the diffusion equation in a uniform medium, it is symmetric in the transverse plane independent of the initial position $\mathbf{x}$. The first-order correction $d^2N_1/d^2\mathbf{p}$ due to the inhomogeneity of the jet transport coefficient $\hat{q}(\mathbf{x})$ as given by Eqs. (45) and (63) is asymmetric in the transverse plane for finite values of the parton's initial position $\mathbf{x}$.

To illustrate the asymmetrical transverse momentum broadening, we show in Fig. 4(a) the first-order correction $d^2N_1/d^2\mathbf{p}$ and in Fig. 4(b) the final transverse momentum

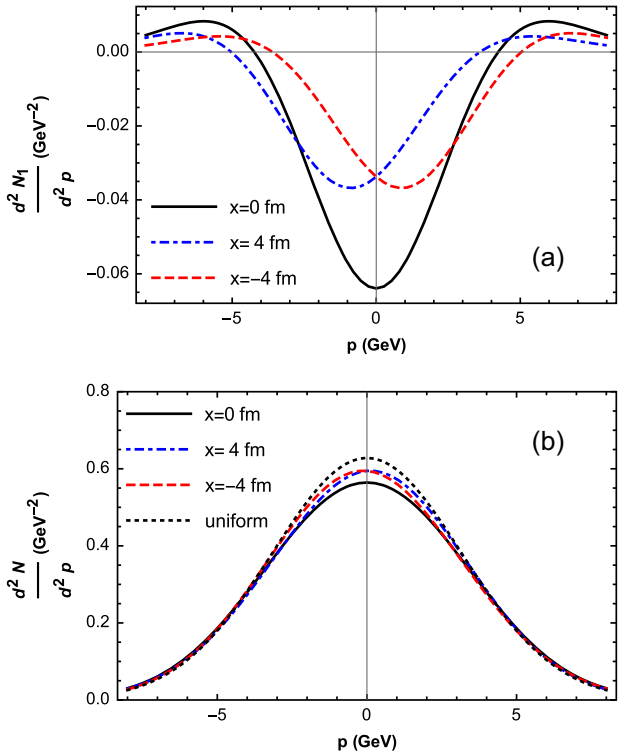

FIG. 4. (a) First-order correction and (b) final transverse momentum distribution for the initial positions $x = -4.0$ fm (red dashed), 0.0 fm (black solid), and 4.0 fm (blue dot-dashed), $\omega = 5$ GeV, $t_f - t_0 = 10$ fm/c, $\hat{q}_0 = 2$ GeV^2/fm, $\delta = 0.1$, and $\sigma = 5$ fm in the simple model for an inhomogeneous jet transport coefficient. The dotted line is the distribution in a uniform medium with a constant jet transport coefficient $\hat{q}_0$.

distribution as a function of $\mathbf{p}\cdot\hat{\mathbf{x}}$ for $\mathbf{p}\cdot(\hat{\mathbf{z}}\times\hat{\mathbf{x}}) = 0$ and different values of the initial position $|\mathbf{x}|$, where $\hat{\mathbf{z}}$ is a unit vector along the initial parton propagation direction. We set $t_f - t_0 = 10$ fm/c, $\sigma = 5$ fm, $\delta = 0.1$, $\hat{q}_0 = 2$ GeV^2/fm, $\omega = 5$ GeV, and $\mathbf{p}_0 = 0$.

In general, the first-order correction in the case we consider here makes the final momentum distribution broader, leading to the increased transverse momentum broadening as compared to that in a uniform medium without a region of inhomogeneity. The distribution is asymmetric for finite values of the initial transverse position of the propagating parton.

One can show that the first-order correction in Eq. (73) does not contribute to the zeroth and first moments of the final transverse momentum distribution, $\int \mathrm{d}^2\mathbf{p} d^2N_1/d^2\mathbf{p} = \int \mathrm{d}^2\mathbf{p}\mathbf{p} d^2N_1/d^2\mathbf{p} = 0$. However, it increases the total transverse momentum broadening,

$$\langle \mathbf{p}^2\rangle = (t_f - t_0)\hat{q}_0 + \langle \Delta\mathbf{p}^2(\mathbf{x}, t_f)\rangle,$$
$$\langle \Delta\mathbf{p}^2(\mathbf{x}, t_f)\rangle = \int_{t_0}^{t_f} \mathrm{d}t \frac{\hat{q}_0\sigma^2\delta}{\Sigma(t)} \exp\left[-\frac{\mathbf{x}^2}{\Sigma(t)}\right], \tag{74}$$

due to the extra density of the medium with inhomogeneity in the region $|x| < \sigma$ on top of a uniform medium. The extra momentum broadening $\langle \Delta\mathbf{p}^2(\mathbf{x}, t_f)\rangle$ due to this region of inhomogeneity grows linearly with time initially when $t_f - t_0 \ll (3\omega^2\sigma^2/\hat{q}_0)^{1/3}$ and saturates at a finite value asymptotically. At $\mathbf{x} = 0$, this finite extra broadening is $\langle \Delta\mathbf{p}^2(\mathbf{0}, t_f)\rangle \approx 1.2\hat{q}_0\delta(3\omega^2\sigma^2/\hat{q}_0)^{1/3}$ when $t_f - t_0 \gg (3\omega^2\sigma^2/\hat{q}_0)^{1/3}$. Compared to the extra momentum broadening in this region of transverse inhomogeneity in a scenario of eikonal propagation without the spatial drifted diffusion in the transverse direction,

$$\langle \mathbf{p}^2(\mathbf{x}, t_f)\rangle_0 = (t_f - t_0)\hat{q}_0 + \langle \Delta\mathbf{p}^2(\mathbf{x}, t_f)\rangle_0,$$
$$\langle \Delta\mathbf{p}^2(\mathbf{x}, t_f)\rangle_0 \approx (t_f - t_0)\hat{q}_0\delta \exp\left[-\frac{\mathbf{x}^2}{\sigma^2}\right], \tag{75}$$

the drifted diffusion in the transverse coordinate due to the transverse gradient reduces the extra momentum broadening in the region of inhomogeneity. In Fig. 5 we show the reduction of the scaled momentum broadening $(\langle \mathbf{p}^2\rangle_0 - \langle \mathbf{p}^2\rangle)/(t_f - t_0)\hat{q}_0\delta = (\langle \Delta\mathbf{p}^2\rangle_0 - \langle \Delta\mathbf{p}^2\rangle)/(t_f - t_0)\hat{q}_0\delta$ as a function of the scaled transverse position $\mathbf{x}/\sigma$ and the scaled propagation time $(t_f - t_0)/(3\omega^2\sigma^2/\hat{q}_0)^{1/3}$. One can see that the reduction becomes significant for a propagation time when the transverse drift distance becomes comparable to the size of the inhomogeneity. Since the inhomogeneity-induced broadening in both scenarios dies out exponentially at large $|\mathbf{x}| > \sigma$ [see Eqs. (74) and (75)], their difference in Fig. 5 also goes to zero exponentially at large $|\mathbf{x}|$.

The first nonvanishing odd moment of the distribution due to the gradient-induced asymmetrical transverse momentum distribution is

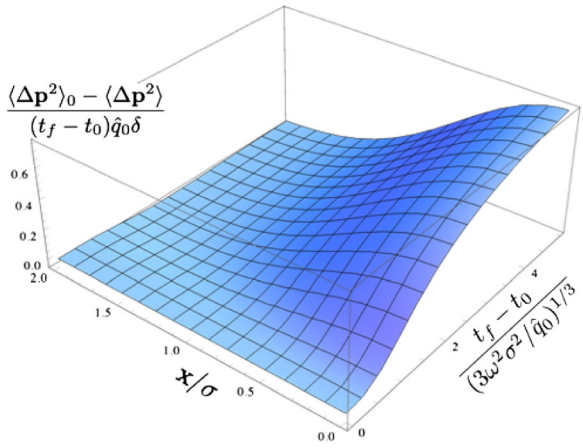

FIG. 5. Reduction of scaled momentum broadening $(\langle \Delta\mathbf{p}^2\rangle_0 - \langle \Delta\mathbf{p}^2\rangle)/(t_f - t_0)\hat{q}_0\delta$ as a function of the scaled transverse position $\mathbf{x}/\sigma$ and propagation time $(t_f - t_0)/(3\omega^2\sigma^2/\hat{q}_0)^{1/3}$.

$$\langle \mathbf{p}^3 \rangle = -2\mathbf{x} \int_{t_0}^{t_f} \mathrm{d}t \frac{\hat{q}_0 \sigma^2 \delta}{\Sigma(t)} \lambda(t) \exp\left\{-\frac{\mathbf{x}^2}{\Sigma(t)}\right\}$$
$$= -\hat{q}_0 \omega \sigma^2 \delta \frac{\mathbf{x}}{\mathbf{x}^2} \left[\exp\left\{-\frac{\mathbf{x}^2}{\sigma^2 + \hat{q}_0 (t_f - t_0)^3/3\omega^2}\right\} - \exp\left\{-\frac{\mathbf{x}^2}{\sigma^2}\right\}\right], \quad (76)$$

which grows initially with the cube of time and saturates at a finite value asymptotically when $(t_f - t_0)^3 \gg 3\omega^2\sigma^2/\hat{q}_0$ because of the finite size of the spatial inhomogeneity.

We can define the transverse asymmetry as proposed in Ref. [49],

$$A_N = \frac{\int \mathrm{d}^2\boldsymbol{Y}\mathrm{d}^2\boldsymbol{p}\mathcal{W}(\boldsymbol{Y},\boldsymbol{p},t_0,t_f)\mathrm{sign}(\hat{\boldsymbol{p}}\cdot\hat{\mathbf{x}})}{\int \mathrm{d}^2\boldsymbol{Y}\mathrm{d}^2\boldsymbol{p}\mathcal{W}(\boldsymbol{Y},\boldsymbol{p},t_0,t_f)}$$
$$= \int \frac{\mathrm{d}^2\boldsymbol{p}}{(2\pi)^2}\frac{d^2N}{d^2\boldsymbol{p}}\mathrm{sign}(\hat{\boldsymbol{p}}\cdot\hat{\mathbf{x}}), \quad (77)$$

to characterize the asymmetrical momentum broadening due to the transverse gradient of the medium. Note that the Wigner function is normalized as $\int \mathrm{d}^2\boldsymbol{Y}d^2\boldsymbol{p}\mathcal{W}(\boldsymbol{Y},\boldsymbol{p},t_0,t_f)/(2\pi)^2 = 1$. Since the asymmetry is only caused by the first-order correction in Eq. (73), one can complete the integration over the transverse momentum and obtain the transverse asymmetry as

$$A_N = \int_{t_0}^{t_f} \mathrm{d}t \frac{\hat{q}_0\sigma^2\delta}{\Sigma(t)\Delta(t)} \frac{\lambda(t)x}{\sqrt{\pi\Delta(t)}} \exp\left\{-\frac{\mathbf{x}^2}{\Sigma(t)} - \frac{\lambda(t)^2\mathbf{x}^2}{\Delta(t)}\right\}. \quad (78)$$

The integration over time can be done numerically. In Fig. 6(a) we show the transverse asymmetry A_N as a function of the initial transverse position x for different values of the parton's energy ω. We note that within the size of the transverse inhomogeneity $|x| < \sigma$, the transverse asymmetry is approximately linear in x driven by the transverse gradient. Conversely, one therefore can use the transverse asymmetry to infer the initial transverse position of the propagating parton. This is the principle underpinning the gradient jet tomography as proposed in Ref. [49]. Combined with the longitudinal jet tomography, which uses the longitudinal momentum of the final jet or parton energy loss to constrain the propagation length, the two-dimensional jet tomography can be used to localize the initial jet production position. Outside the range of the medium inhomogeneity $|x| > \sigma$, the transverse asymmetry decreases and vanishes when the transverse gradient decreases.

Similar to the second and third moments of the momentum distribution, the transverse asymmetry A_N also increases with the propagation time during the diffusion across the domain of the inhomogeneity. Since

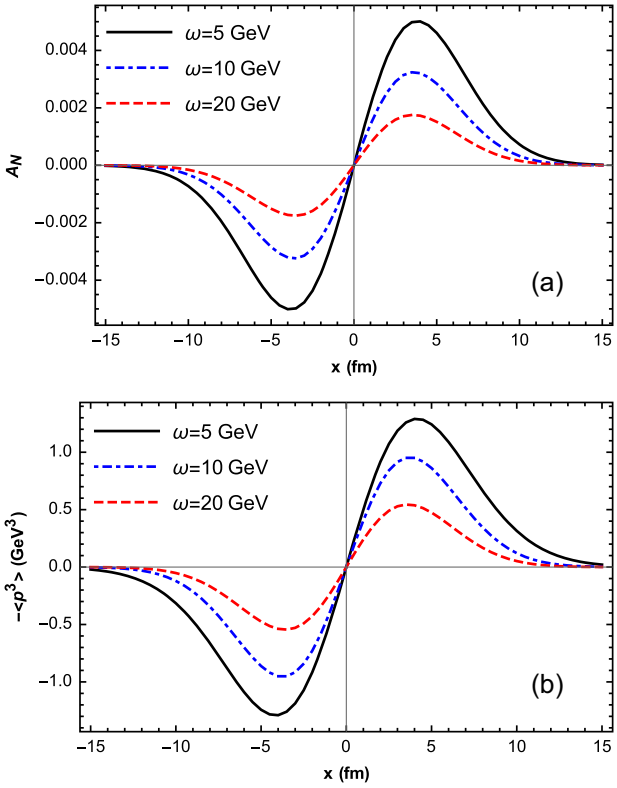

FIG. 6. (a) Transverse momentum asymmetry and (b) third moment of the transverse momentum distribution as a function of the initial transverse position x for $t_f - t_0 = 10$ fm/c, $\hat{q}_0 = 2$ GeV^2/fm, $\delta = 0.1$, and $\sigma = 5$ fm in the simple model.

$\sqrt{\hat{q}_0(t_f - t_0)}/\omega$ is the average diffusion velocity, $\sqrt{\hat{q}_0(t_f - t_0)^3}/\omega$ is the diffusion distance during the propagation time. When this distance is much larger than the size of the inhomogeneity σ or $(t_f - t_0)^3 \gg \omega^2\sigma^2/\hat{q}_0$, the transverse asymmetry as well as the increased momentum broadening $\langle \Delta\mathbf{p}^2 \rangle$ and the third moment $\langle \mathbf{p}^3 \rangle$ will saturate to the asymptotic values. Since the average diffusion distance is inversely proportional to the parton's energy ω, the transverse asymmetry A_N, as well as the third moment and the extra momentum broadening, decrease with ω.

In Fig. 6(b), we also plot the third moment $\langle \mathbf{p}^3 \rangle$ as a function of the initial transverse position x. It has the same behavior as the transverse asymmetry. As seen in Fig. 4(a), the first-order correction to the distribution changes sign at large transverse momentum. The third moment has a much larger weight at large transverse momentum and is therefore dominated by the first-order correction in this large-momentum region. Therefore, the asymmetry as characterized by the third moment has the opposite sign as the transverse asymmetry A_N, which is dominated by the distribution at small momentum. However, their dependence on the initial transverse position x, the propagation time $t_f - t_0$, and energy ω is the same.

V. SUMMARY

To demonstrate the principle of the gradient tomography in jet quenching, we have derived the evolution of the Wigner distribution function in transverse momentum and coordinate for a fast parton traveling inside a strong interaction medium within the path-integral approach. Within the dipole approximation for soft multiple scatterings in the medium encoded in the correlation of Wilson operators, the evolution can be expressed generally in terms of a Green function or the evolution operator, which is determined by the space-time profile of the jet transport coefficient $\hat{q}$.

In a uniform medium with a constant jet transport coefficient $\hat{q}_0$, one can complete the path integral and obtain the evolution operator and the corresponding Wigner distribution analytically which is also a solution to a drift-diffusion Boltzmann transport equation. We also considered a special case of an inhomogeneous medium by assuming a form of a spatially dependent jet transport coefficient that adds a Gaussian-like region of enhanced medium density with a finite size. The path integral can also be completed in this case, and we obtained the evolution operator analytically. We have considered an initial condition for a classical point-like particle and calculated the final transverse momentum distribution and its dependence on the initial transverse coordinate. The distribution is asymmetric when the initial position of the parton is not at the center of the Gaussian-like region because of the transverse gradient. The Gaussian-like inhomogeneity was found to increase the momentum broadening $\langle \mathbf{p}^2 \rangle$ and lead to a nonvanishing value of the odd moment $\langle \mathbf{p}^3 \rangle$ due to the asymmetrical distribution. We also calculated the transverse asymmetry A_N as proposed in the study of the gradient tomography [49]. We found that both A_N and $\langle \mathbf{p}^3 \rangle$ are linearly correlated with the initial transverse position within the region of the inhomogeneity, validating the principle of the gradient jet tomography. This analytical solution also allowed us to understand both the propagation time (length) and energy dependence of the transverse asymmetry.

We would like to point out that the two setups—a static and uniform medium and a static medium with only transverse inhomogeneity—were considered in our study because they enabled us to complete the path integral analytically. A similar setup for the medium was also considered in recent analytical work on the jet broadening in an inhomogeneous medium in Refs. [57,58]. In addition, we should also note that the inhomogeneity of the jet transport coefficient in Eq. (64) is assumed to be small, which enables us to use the perturbative expansion and complete the path integral in the calculation of the Wigner function. This leads to small numerical values of the transverse momentum asymmetry. In real heavy-ion collisions, the QGP medium is inhomogeneous in both the transverse and longitudinal directions of the parton propagation with large gradients. It also evolves with time. The asymmetry from the semiclassical Boltzmann transport is very large and can be used for the purpose of gradient tomography, as shown in Ref. [49]. The recent study using deep-learning-assisted jet tomography to select events with specified regions of the initial jet production in Ref. [65] explicitly showed that the asymmetrical momentum (or azimuthal angle) distribution is closely related to the inhomogeneity as well as the radial flow of the medium.

Although the study of asymmetrical transverse momentum broadening in a more realistic scenario within the path-integral approach is our final goal, it is beyond the scope of this paper. Going beyond the simple form of the spatially dependent jet transport coefficient and considering the realistic case of parton propagation in heavy-ion collisions, numerical evaluation of the path integral for more realistic cases of the medium is needed. However, our study in this paper using simplified geometries of the QGP medium demonstrates the principle of gradient jet tomography within the path-integral formulation.

Since the path-integral approach differs from the classical transport approach in which one can also introduce space and time dependences of the jet transport coefficient in the drift-diffusion Boltzmann equation (as was done in Ref. [49]), it will also be interesting to examine the difference between the two approaches. These studies will help to establish the gradient jet tomography as a powerful tool to explore properties of QGP using jet quenching.

ACKNOWLEDGMENTS

We thank Yayun He and Longgang Pang for helpful discussions. This work is supported in part by the National Natural Science Foundation of China (NSFC) under Grant Nos. 11935007, 11861131009, and 11890714; by the Director, Office of Energy Research, Office of High Energy and Nuclear Physics, Division of Nuclear Physics, of the U.S. Department of Energy under Contract No. DE-AC02-05CH11231; by the US National Science Foundation under Grant No. ACI-1550228 within JETSCAPE and OAC-2004571 within the X-SCAPE Collaboration; and by the Grants SGR-2017-754, PID2019–105614GB-C21, and PID2019–105614GB-C22 and the "Unit of Excellence MdM 2020-2023" award to the Institute of Cosmos Sciences (CEX2019-000918-M).

APPENDIX A: FUNCTIONAL MEASURE

Let us consider the calculation of the propagator in one-dimensional space. We divide the computation into many steps; inserting the closure relation many times, we write the propagator as the products of the propagators with a small time interval,

$$\begin{aligned}\langle x_f|e^{-iH(t_f-t_0)}|x_0\rangle &= \lim_{\epsilon\to 0}\langle x_f|e^{-iH\epsilon}e^{-iH\epsilon}\ldots e^{-iH\epsilon}|x_0\rangle \\ &= \prod_{i=1}^{N-1}\int \mathrm{d}x_i \langle x_f|e^{-iH\epsilon}|x_{N-1}\rangle \\ &\quad\times\langle x_{N-1}|e^{-iH\epsilon}|x_{N-2}\rangle \\ &\quad\cdots\langle x_2|e^{-iH\epsilon}|x_1\rangle\langle x_1|e^{-iH\epsilon}|x_0\rangle. \end{aligned} \tag{A1}$$

We also insert the identity operator which runs over all momentum states in the propagator,

$$\langle x_{i+1}|e^{-iH\epsilon}|x_i\rangle = \int \mathrm{d}p_i \langle x_{i+1}|p_i\rangle\langle p_i|e^{-iH\epsilon}|x_i\rangle = \int \mathrm{d}p_i \frac{e^{ip_i x_{i+1}}}{\sqrt{2\pi}}\langle p_i|e^{-iH\epsilon}|x_i\rangle. \tag{A2}$$

If we suppose that H takes the form $H(x,p)=\frac{p^2}{2m}+V(x)$, in the limit $\epsilon=\frac{t_f-t_0}{N}\to 0$ we have

$$\exp\left[i\left(\frac{p^2}{2m}+V(x)\right)\epsilon\right] \approx \exp\left[i\frac{p^2}{2m}\epsilon\right]\exp[iV(x)\epsilon], \tag{A3}$$

or

$$\langle p_i|H|x_i\rangle = \langle p_i|x_i\rangle H(x_i,p_i). \tag{A4}$$

The propagator in Eq. (A2) can be written as

$$\begin{aligned}\langle x_{i+1}|e^{-iH\epsilon}|x_i\rangle &= \int \frac{\mathrm{d}p_i}{2\pi} e^{ip_i(x_{i+1}-x_i)-iH(x_i,p_i)\epsilon} \\ &= \int \frac{\mathrm{d}p_i}{2\pi}\exp\left\{i\epsilon\left(p_i\dot{x}_i-\frac{p_i^2}{2m}-V(x_i)\right)\right\} \\ &= \sqrt{\frac{m}{2\pi i\epsilon}}\exp\left\{i\epsilon\left(\frac{m}{2}\dot{x}_i^2-V(x_i)\right)\right\} \\ &\equiv \sqrt{\frac{m}{2\pi i\epsilon}}\exp\{i\epsilon L(x_i,\dot{x}_i)\}.\end{aligned} \tag{A5}$$

Using the above equation for each time interval in Eq. (A1), one can get the path integral in the form $\int \mathcal{D}x e^{iS}$, with the functional measure defined as

$$\mathcal{D}x = \sqrt{\frac{m}{2\pi i\epsilon}}\prod_{i=1}^{N-1}\sqrt{\frac{m}{2\pi i\epsilon}}dx_i. \tag{A6}$$

Replacing $m\to\omega$, we have $A=\sqrt{\frac{2\pi i\epsilon}{\omega}}$ in Eq. (15).

APPENDIX B: NORMALIZATION OF GAUSSIAN DISTRIBUTION

The discrete version of the classical trajectory of the hard parton $\boldsymbol{R}$ in Eq. (33) can be cast as

$$\boldsymbol{R}_j = \boldsymbol{X} + j\epsilon\frac{\boldsymbol{p}_0}{\omega}+\frac{\epsilon^2}{\omega}\sum_{i=1}^{j-1}(j-i)\boldsymbol{\xi}_i. \tag{B1}$$

In this expression, $\boldsymbol{R}_j$ depends only on $\boldsymbol{\xi}_i$ with $i<j$ so that

$$\int \mathrm{d}^2\boldsymbol{\xi}_j\left(\frac{\epsilon}{\pi}\right)\frac{1}{\hat{q}(\boldsymbol{R}_j)}\exp\left\{-\epsilon\frac{\boldsymbol{\xi}_j^2}{\hat{q}(\boldsymbol{R}_j)}\right\}=1. \tag{B2}$$

Since $\hat{q}(\boldsymbol{R}_j)$ is a function of $\boldsymbol{\xi}_i$ with $i<j$ and does not depend on $\boldsymbol{\xi}_j$, the integrand is just a trivial Gaussian form. Then, we get

$$\int \mathcal{D}\boldsymbol{\xi}\frac{1}{\det\{\hat{q}(\boldsymbol{R})\}}\exp\left\{-\int_{t_0}^{t_f}\mathrm{d}t\frac{\boldsymbol{\xi}^2(t)}{\hat{q}(\boldsymbol{R})}\right\} = \prod_{j=1}^{N-1}\int \mathrm{d}^2\boldsymbol{\xi}_j\left(\frac{\epsilon}{\pi}\right)\frac{1}{\hat{q}(\boldsymbol{R}_j)}\exp\left\{-\epsilon\frac{\boldsymbol{\xi}_j^2}{\hat{q}(\boldsymbol{R}_j)}\right\}=1. \tag{B3}$$

APPENDIX C: CORRELATION FUNCTIONS

We define the generating function

$$Z[\boldsymbol{J}(t)] \equiv \int \mathcal{D}\boldsymbol{\xi}(t)\frac{1}{\det\{\hat{q}(\boldsymbol{R})\}}\exp\left\{-\int \mathrm{d}t\frac{\boldsymbol{\xi}^2(t)}{\hat{q}(\boldsymbol{R})}\right\} \times \exp\left\{\int \mathrm{d}t\boldsymbol{J}(t)\cdot\boldsymbol{\xi}(t)\right\}, \tag{C1}$$

and the corresponding discretization version is

$$Z[\boldsymbol{J}(t)] = \prod_{j=1}^{N-1}\int \mathrm{d}^2\boldsymbol{\xi}_j\left(\frac{\epsilon}{\pi}\right)\frac{1}{\hat{q}(\boldsymbol{R}_j)}\exp\left\{-\epsilon\frac{\boldsymbol{\xi}_j^2}{\hat{q}(\boldsymbol{R}_j)}\right\} \times \exp\{-\epsilon\boldsymbol{J}_j\cdot\boldsymbol{\xi}_j\}, \tag{C2}$$

which encodes all correlation functions.

In the case of a constant $\hat{q}(\boldsymbol{R})=\hat{q}_0$ in a uniform medium, differentiating $Z[\boldsymbol{J}(t)]$ with respect to $\boldsymbol{J}(t)$ evaluated at some time $t=t_1$ leads to

$$\frac{\delta Z}{\delta J^a(t_1)}|_{J=0} = \int \mathcal{D}\boldsymbol{\xi}(t)\frac{1}{\det\{\hat{q}_0\}}\exp\left\{-\int \mathrm{d}t\frac{\boldsymbol{\xi}(t)^2}{\hat{q}_0}\right\}\xi^a(t_1) = \langle\xi^a(t_1)\rangle_0. \tag{C3}$$

In the same spirit, taking n derivatives gives us

$$\begin{aligned}&\frac{\delta^n Z}{\delta J^{a_1}(t_1)\delta J^{a_2}(t_2)\cdots\delta J^{a_n}(t_n)}\bigg|_{J=0} \\ &= \int \mathcal{D}\boldsymbol{\xi}(t)\frac{1}{\det\{\hat{q}_0\}}\exp\left\{-\int \mathrm{d}t\frac{\boldsymbol{\xi}(t)^2}{\hat{q}_0}\right\}\xi^{a_1}(t_1)\cdots\xi^{a_n}(t_n) \\ &= \langle\xi^{a_1}(t_1)\xi^{a_2}(t_2)\cdots\xi^{a_n}(t_n)\rangle_0.\end{aligned} \tag{C4}$$

The generating function above is just a functional Gaussian integral, which can be performed exactly. This leads us to

$$Z[\boldsymbol{J}(t)] = \int \mathcal{D}\boldsymbol{\xi}(t)\frac{1}{\det\{\hat{q}_0\}}\exp\left\{-\int \mathrm{d}t\frac{1}{\hat{q}_0}\left(\boldsymbol{\xi}(t)-\frac{\hat{q}_0}{2}\boldsymbol{J}\right)^2\right\} \times \exp\left\{\int \mathrm{d}t\frac{\hat{q}_0}{4}\boldsymbol{J}^2\right\} = \exp\left\{\int \mathrm{d}t\frac{\hat{q}_0}{4}\boldsymbol{J}^2\right\}. \tag{C5}$$

Taking derivatives with respect to J^a, we have

$$\begin{aligned}\frac{\delta Z}{\delta J^a(t_1)} &= \frac{\hat{q}_0}{2}J^a(t_1)Z[\boldsymbol{J}] \\ \frac{\delta^2 Z}{\delta J^a(t_1)\delta J^b(t_2)} &= \frac{\hat{q}_0}{2}\delta^{ab}\delta(t_1-t_2)Z[\boldsymbol{J}] \\ &\quad + \frac{\hat{q}_0^2}{4}J^a(t_1)J^b(t_2)Z[\boldsymbol{J}].\end{aligned} \tag{C6}$$

Setting $\boldsymbol{J}=\boldsymbol{0}$, we get

$$\langle\xi^a(t_1)\rangle_0=\left.\frac{\delta Z}{\delta J^a(t_1)}\right|_{\boldsymbol{J}=\boldsymbol{0}}=0,$$
$$\langle\xi^a(t_1)\xi^b(t_2)\rangle_0=\left.\frac{\delta^2 Z}{\delta J^a(t_1)\delta J^b(t_2)}\right|_{\boldsymbol{J}=\boldsymbol{0}}=\frac{\hat{q}_0}{2}\delta^{ab}\delta(t_1-t_2). \tag{C7}$$

Note that when $\hat{q}=\hat{q}(\boldsymbol{R})$ but is not a constant ($\hat{q}_0$), we do not have such simple expressions for two-point functions. Since $\boldsymbol{R}_{N-1}$ is $\boldsymbol{\xi}_{N-2}$ dependent, we can not perform the above path integral in the generating function (C1) exactly.

APPENDIX D: SPECTRA IN A UNIFORM MEDIUM

For a uniform medium, one can complete the following path integral by taking advantage of the two-point correlation function in Eq. (28):

$$\left\langle\exp\left\{i\boldsymbol{x}\cdot\int_{t_0}^{t_f}\mathrm{d}t\boldsymbol{\xi}(t)\right\}\right\rangle_0\equiv\int\widehat{\mathcal{D}}\boldsymbol{\xi}\exp\left\{i\boldsymbol{x}\cdot\int_{t_0}^{t_f}\mathrm{d}t\boldsymbol{\xi}(t)-\int_{t_0}^{t_f}\mathrm{d}t\frac{\boldsymbol{\xi}(t)^2}{\hat{q}_0}\right\}$$
$$=\int\widehat{\mathcal{D}}\boldsymbol{\xi}\exp\left\{-\int_{t_0}^{t_f}\mathrm{d}t\frac{1}{\hat{q}_0}\left[\boldsymbol{\xi}(t)-i\frac{\hat{q}_0}{2}\boldsymbol{x}\right]^2-\int_{t_0}^{t_f}\mathrm{d}t\frac{\hat{q}_0}{4}\boldsymbol{x}^2\right\}=\exp\left\{-\int_{t_0}^{t_f}\mathrm{d}t\frac{\hat{q}_0}{4}\boldsymbol{x}^2\right\}. \tag{D1}$$

According to Eq. (37), we have

$$\frac{d^2N}{d^2\boldsymbol{p}}=\int\mathrm{d}^2\boldsymbol{X}\mathrm{d}^2\boldsymbol{p}_0\frac{\mathrm{d}^2\boldsymbol{x}}{(2\pi)^2}\mathcal{W}(\boldsymbol{X},\boldsymbol{p}_0;t_0,t_0)e^{-i\boldsymbol{x}\cdot(\boldsymbol{p}-\boldsymbol{p}_0)}\exp\left\{-\int_{t_0}^{t_f}\mathrm{d}t\frac{\hat{q}_0}{4}\boldsymbol{x}^2\right\}, \tag{D2}$$

which leads to Eq. (39) after integrating over $\boldsymbol{x}$. Similarly, one can get

$$\left\langle\exp\left\{i\boldsymbol{x}\cdot\int_{t_0}^{t_f}\mathrm{d}t'\int_{t_0}^{t'}\mathrm{d}t''\frac{\boldsymbol{\xi}(t'')}{t_f-t_0}\right\}\right\rangle_0=\exp\left\{-\int_{t_0}^{t_f}\mathrm{d}t\frac{\hat{q}_0}{12}\boldsymbol{x}^2\right\}, \tag{D3}$$

$$\left\langle\exp\left\{i(\boldsymbol{x}-\boldsymbol{y})\cdot\int_{t_0}^{t_f}\mathrm{d}t'\int_{t_0}^{t'}\mathrm{d}t''\frac{\boldsymbol{\xi}(t'')}{t_f-t_0}+i\boldsymbol{y}\cdot\int_{t_0}^{t_f}\mathrm{d}t'\boldsymbol{\xi}(t')\right\}\right\rangle_0=\exp\left\{-\left(\int_{t_0}^{t_f}\mathrm{d}t\frac{\hat{q}_0}{12}(\boldsymbol{x}-\boldsymbol{y})^2+\int_{t_0}^{t_f}\mathrm{d}t\frac{\hat{q}_0}{4}\boldsymbol{x}\cdot\boldsymbol{y}\right)\right\}, \tag{D4}$$

and then arrive at Eqs. (40) and (38) as well.

APPENDIX E: LEADING-ORDER (IN f) APPROXIMATION OF THE FUNCTIONAL INTEGRAL F

With the variable transformation $\boldsymbol{\xi}'=\boldsymbol{\xi}-i\frac{\hat{q}_0}{2}\boldsymbol{x}$,

$$F(\boldsymbol{x},\boldsymbol{X},\boldsymbol{p}_0)$$
$$=\exp\left\{-\int_{t_0}^{t_f}\mathrm{d}t\frac{\hat{q}_0}{4}\boldsymbol{x}^2\right\}\int\mathcal{D}\boldsymbol{\xi}'\frac{\det\{1-f(\boldsymbol{R})\}}{\det\{\hat{q}_0\}}\exp\left\{\int_{t_0}^{t_f}\mathrm{d}t\left[\frac{\boldsymbol{\xi}'(t)^2}{\hat{q}_0}+i\boldsymbol{x}\cdot\boldsymbol{\xi}'(t)-\frac{\hat{q}_0}{4}\boldsymbol{x}^2\right]f(\boldsymbol{R})\right\}\exp\left\{-\int_{t_0}^{t_f}\mathrm{d}t\frac{\boldsymbol{\xi}'(t)^2}{\hat{q}_0}\right\}$$
$$=\exp\left\{-\int_{t_0}^{t_f}\mathrm{d}t\frac{\hat{q}_0}{4}\boldsymbol{x}^2\right\}\prod_{k=1}^{N-1}\int\left(\frac{\epsilon}{\pi}\right)d^2\boldsymbol{\xi}_k'\frac{1-f(\boldsymbol{R}_k)}{\hat{q}_0}\exp\left\{\epsilon\left[\frac{\boldsymbol{\xi}_k'^2}{\hat{q}_0}+i\boldsymbol{x}\cdot\boldsymbol{\xi}_k'-\frac{\hat{q}_0}{4}\boldsymbol{x}^2\right]f(\boldsymbol{R}_k)\right\}\exp\left\{-\epsilon\frac{\boldsymbol{\xi}_k'^2}{\hat{q}_0}\right\}, \tag{E1}$$

where $\epsilon\to0$ and $N\to\infty$. It can be approximately rewritten, to the leading order in f, as

$$F(\boldsymbol{x},\boldsymbol{X},\boldsymbol{p}_0)\approx\exp\left\{-\int_{t_0}^{t_f}\mathrm{d}t\frac{\hat{q}_0}{4}\boldsymbol{x}^2\right\}\prod_{k=1}^{N-1}\int\left(\frac{\epsilon}{\pi}\right)d^2\boldsymbol{\xi}_k'\frac{1}{\hat{q}_0}\left\{1+\epsilon\left[\frac{\boldsymbol{\xi}_k'^2}{\hat{q}_0}+i\boldsymbol{x}\cdot\boldsymbol{\xi}_k'-\frac{\hat{q}_0}{4}\boldsymbol{x}^2-\frac{1}{\epsilon}\right]f(\boldsymbol{R}_k)\right\}\exp\left\{-\epsilon\frac{\boldsymbol{\xi}_k'^2}{\hat{q}_0}\right\}$$
$$=\exp\left\{-\int_{t_0}^{t_f}\mathrm{d}t\frac{\hat{q}_0}{4}\boldsymbol{x}^2\right\}\int\mathcal{D}\boldsymbol{\xi}'\frac{1}{\det\{\hat{q}_0\}}\left\{1+\int_{t_0}^{t_f}\mathrm{d}t\left[\frac{\boldsymbol{\xi}'(t)^2}{\hat{q}_0}+i\boldsymbol{x}\cdot\boldsymbol{\xi}'(t)-\frac{\hat{q}_0}{4}\boldsymbol{x}^2-\frac{1}{\epsilon}\right]f(\boldsymbol{R})\right\}\exp\left\{-\int_{t_0}^{t_f}\mathrm{d}t\frac{\boldsymbol{\xi}'(t)^2}{\hat{q}_0}\right\}$$
$$\equiv\exp\left\{-\int_{t_0}^{t_f}\mathrm{d}t\frac{\hat{q}_0}{4}\boldsymbol{x}^2\right\}\left\{1+\int_{t_0}^{t_f}\mathrm{d}t\left\langle\left[\frac{\boldsymbol{\xi}'(t)^2}{\hat{q}_0}+i\boldsymbol{x}\cdot\boldsymbol{\xi}'(t)-\frac{\hat{q}_0}{4}\boldsymbol{x}^2-\frac{1}{\epsilon}\right]f(\boldsymbol{R}(t,\boldsymbol{\xi}'(t))\right\rangle_0\right\}. \tag{E2}$$

Using the expansion of $f(\boldsymbol{R})$ [see Eq. (51)] and the correlators

$$\langle[\boldsymbol{\xi}'(t)]^2\rangle_0 \equiv \int \widehat{\mathcal{D}}\boldsymbol{\xi}' \exp\left\{-\int_{t_0}^{t_f} \mathrm{d}t \frac{\boldsymbol{\xi}'(t)^2}{\hat{q}_0}\right\} \boldsymbol{\xi}'(t)^2 = \hat{q}_0\delta(t-t), \tag{E3}$$

$$\langle[\boldsymbol{\xi}'(t)]^2\Delta R^i(t,\boldsymbol{\xi}')\rangle_0 = \int \widehat{\mathcal{D}}\boldsymbol{\xi}' \exp\left\{-\int_{t_0}^{t_f} \mathrm{d}t \frac{\boldsymbol{\xi}'(t)^2}{\hat{q}_0}\right\} \frac{1}{\omega}\int_{t_0}^{t} \mathrm{d}t_1 (t-t_1)\boldsymbol{\xi}'(t)^2 \xi'^i(t_1) = 0, \tag{E4}$$

$$\langle[\boldsymbol{\xi}'(t)]^2\Delta R^i(t,\boldsymbol{\xi}')\Delta R^j(t,\boldsymbol{\xi}')\rangle_0 = \langle[\boldsymbol{\xi}'(t)]^2\rangle_0 \langle\Delta R^i(t,\boldsymbol{\xi}')\Delta R^j(t,\boldsymbol{\xi}')\rangle_0, \tag{E5}$$

$$\langle[\boldsymbol{\xi}'(t)]^2\Delta R^{i_1}(t,\boldsymbol{\xi}')\Delta R^{i_2}(t,\boldsymbol{\xi}')\Delta R^{i_3}(t,\boldsymbol{\xi}')\Delta R^{i_4}(t,\boldsymbol{\xi}')\cdots\Delta R^{i_{2n-1}}(t,\boldsymbol{\xi}')\rangle_0 = 0, \tag{E6}$$

$$\langle[\boldsymbol{\xi}'(t)]^2\Delta R^{i_1}(t,\boldsymbol{\xi}')\Delta R^{i_2}(t,\boldsymbol{\xi}')\cdots\Delta R^{i_{2n}}(t,\boldsymbol{\xi}')\rangle_0 = \langle[\boldsymbol{\xi}'(t)]^2\rangle_0 \langle\Delta R^{i_1}(t,\boldsymbol{\xi}')\Delta R^{i_2}(t,\boldsymbol{\xi}')\cdots\Delta R^{i_{2n}}(t,\boldsymbol{\xi}')\rangle_0, \tag{E7}$$

we arrive at

$$\begin{aligned} F(\boldsymbol{x},\boldsymbol{X},\boldsymbol{p}_0) &= \exp\left\{-\int_{t_0}^{t_f} \mathrm{d}t \frac{\hat{q}_0}{4}\boldsymbol{x}^2\right\}\left[1+\int_{t_0}^{t_f} \mathrm{d}t\left[\frac{\hat{q}_0\delta(t-t)}{\hat{q}_0} - \frac{\hat{q}_0}{4}\boldsymbol{x}^2 - \frac{1}{\epsilon}\right]\langle f(\boldsymbol{R}(t,\boldsymbol{\xi}'(t))\rangle_0\right] \\ &= \exp\left\{-\int_{t_0}^{t_f} \mathrm{d}t \frac{\hat{q}_0}{4}\boldsymbol{x}^2\right\}\left[1-\int_{t_0}^{t_f} \mathrm{d}t \frac{\hat{q}_0}{4}\boldsymbol{x}^2\langle f(\boldsymbol{R}(t,\boldsymbol{\xi}'(t))\rangle_0 + \sum_{k=1}^{N-1}\delta_{kk} - \sum_{k=1}^{N-1}\epsilon\frac{1}{\epsilon}\right] \\ &= \exp\left\{-\int_{t_0}^{t_f} \mathrm{d}t \frac{\hat{q}_0}{4}\boldsymbol{x}^2\right\}\left[1-\int_{t_0}^{t_f} \mathrm{d}t \frac{\hat{q}_0}{4}\boldsymbol{x}^2\langle f(\boldsymbol{R}(t,\boldsymbol{\xi}'(t))\rangle_0\right], \end{aligned} \tag{E8}$$

where we have used $\int \mathrm{d}x g(x)\delta(x-x') = g(x'\equiv x_i) = \sum_{k=1}^{N-1} g(x_k)\delta_{ki}$ for a smooth function $g(x)$.

[1] K. Adcox *et al.* (PHENIX Collaboration), Nucl. Phys. **A757**, 184 (2005).
[2] I. Arsene *et al.* (BRAHMS Collaboration), Nucl. Phys. **A757**, 1 (2005).
[3] B. B. Back *et al.* (PHOBOS Collaboration), Nucl. Phys. **A757**, 28 (2005).
[4] J. Adams *et al.* (STAR Collaboration), Nucl. Phys. **A757**, 102 (2005).
[5] M. Gyulassy and M. Plumer, Phys. Lett. B **243**, 432 (1990).
[6] X.-N. Wang and M. Gyulassy, Phys. Rev. Lett. **68**, 1480 (1992).
[7] K. Adcox *et al.* (PHENIX Collaboration), Phys. Rev. Lett. **88**, 022301 (2002).
[8] C. Adler *et al.* (STAR Collaboration), Phys. Rev. Lett. **89**, 202301 (2002).
[9] G. Aad *et al.* (ATLAS Collaboration), Phys. Rev. Lett. **105**, 252303 (2010).
[10] S. Chatrchyan *et al.* (CMS Collaboration), Phys. Rev. C **84**, 024906 (2011).
[11] K. Aamodt *et al.* (ALICE Collaboration), Phys. Lett. B **696**, 30 (2011).
[12] G. Aad *et al.* (ATLAS Collaboration), Phys. Lett. B **719**, 220 (2013).
[13] M. Aaboud *et al.* (ATLAS Collaboration), Phys. Lett. B **790**, 108 (2019).
[14] M. Gyulassy and X.-N. Wang, Nucl. Phys. **B420**, 583 (1994).
[15] R. Baier, Y. L. Dokshitzer, A. H. Mueller, S. Peigne, and D. Schiff, Nucl. Phys. **B483**, 291 (1997).
[16] R. Baier, Y. L. Dokshitzer, A. H. Mueller, S. Peigne, and D. Schiff, Nucl. Phys. **B484**, 265 (1997).
[17] R. Baier, Y. L. Dokshitzer, A. H. Mueller, and D. Schiff, Nucl. Phys. **B531**, 403 (1998).
[18] B. G. Zakharov, JETP Lett. **63**, 952 (1996).
[19] B. G. Zakharov, JETP Lett. **65**, 615 (1997).
[20] B. G. Zakharov, Phys. At. Nucl. **61**, 838 (1998).
[21] M. Gyulassy, P. Levai, and I. Vitev, Phys. Rev. Lett. **85**, 5535 (2000).
[22] M. Gyulassy, P. Levai, and I. Vitev, Nucl. Phys. **B594**, 371 (2001).
[23] U. A. Wiedemann, Nucl. Phys. **B582**, 409 (2000).
[24] U. A. Wiedemann, Nucl. Phys. **B588**, 303 (2000).
[25] A. Kovner and U. A. Wiedemann, *Quark Gluon Plasma 3*, edited by Rudolph C. Hwa and Xin-Nian Wang (World Scientific, Singapore, 2003), p. 192.
[26] C. A. Salgado and U. A. Wiedemann, Phys. Rev. Lett. **89**, 092303 (2002).

[27] N. Armesto, C. A. Salgado, and U. A. Wiedemann, Phys. Rev. Lett. **94**, 022002 (2005).
[28] P. B. Arnold, G. D. Moore, and L. G. Yaffe, J. High Energy Phys. 11 (2001) 057.
[29] P. B. Arnold, G. D. Moore, and L. G. Yaffe, J. High Energy Phys. 12 (2001) 009.
[30] P. B. Arnold, G. D. Moore, and L. G. Yaffe, J. High Energy Phys. 06 (2002) 030.
[31] X.-F. Guo and X.-N. Wang, Phys. Rev. Lett. **85**, 3591 (2000).
[32] X.-N. Wang and X.-F. Guo, Nucl. Phys. **A696**, 788 (2001).
[33] X.-F. Chen, C. Greiner, E. Wang, X.-N. Wang, and Z. Xu, Phys. Rev. C **81**, 064908 (2010).
[34] K. M. Burke *et al.* (JET Collaboration), Phys. Rev. C **90**, 014909 (2014).
[35] S. Cao *et al.* (JETSCAPE Collaboration), Phys. Rev. C **104**, 024905 (2021).
[36] M. L. Miller, K. Reygers, S. J. Sanders, and P. Steinberg, Annu. Rev. Nucl. Part. Sci. **57**, 205 (2007).
[37] X.-N. Wang, Phys. Rev. C **63**, 054902 (2001).
[38] M. Gyulassy, I. Vitev, and X. N. Wang, Phys. Rev. Lett. **86**, 2537 (2001).
[39] M. Gyulassy, I. Vitev, X.-N. Wang, and P. Huovinen, Phys. Lett. B **526**, 301 (2002).
[40] B. Betz, M. Gyulassy, and G. Torrieri, Phys. Rev. C **84**, 024913 (2011).
[41] D. Zigic, I. Salom, J. Auvinen, M. Djordjevic, and M. Djordjevic, Phys. Lett. B **791**, 236 (2019).
[42] C. Andres, N. Armesto, H. Niemi, R. Paatelainen, and C. A. Salgado, Phys. Lett. B **803**, 135318 (2020).
[43] J. Noronha-Hostler, B. Betz, J. Noronha, and M. Gyulassy, Phys. Rev. Lett. **116**, 252301 (2016).
[44] J. Xu, J. Liao, and M. Gyulassy, J. High Energy Phys. 02 (2016) 169.
[45] S. Shi, J. Liao, and M. Gyulassy, Chin. Phys. C **43**, 044101 (2019).
[46] Y. He, W. Chen, T. Luo, S. Cao, L.-G. Pang, and X.-N. Wang, Phys. Rev. C **106**, 044904 (2022).
[47] H. Zhang, J. F. Owens, E. Wang, and X.-N. Wang, Phys. Rev. Lett. **98**, 212301 (2007).
[48] H. Zhang, J. F. Owens, E. Wang, and X.-N. Wang, Phys. Rev. Lett. **103**, 032302 (2009).
[49] Y. He, L.-G. Pang, and X.-N. Wang, Phys. Rev. Lett. **125**, 122301 (2020).
[50] Z. Yang, W. Chen, Y. He, W. Ke, L. Pang, and X.-N. Wang, Phys. Rev. Lett. **127**, 082301 (2021).
[51] H. Li, F. Liu, G.-l. Ma, X.-N. Wang, and Y. Zhu, Phys. Rev. Lett. **106**, 012301 (2011).
[52] X.-N. Wang and Y. Zhu, Phys. Rev. Lett. **111**, 062301 (2013).
[53] Y. He, T. Luo, X.-N. Wang, and Y. Zhu, Phys. Rev. C **91**, 054908 (2015); **97**, 019902(E) (2018).
[54] T. Luo, S. Cao, Y. He, and X.-N. Wang, Phys. Lett. B **782**, 707 (2018).
[55] E. P. Wigner, Phys. Rev. **40**, 749 (1932).
[56] M. Hillery, R. F. O'Connell, M. O. Scully, and E. P. Wigner, Phys. Rep. **106**, 121 (1984).
[57] A. V. Sadofyev, M. D. Sievert, and I. Vitev, Phys. Rev. D **104**, 094044 (2021).
[58] J. a. Barata, A. V. Sadofyev, and C. A. Salgado, Phys. Rev. D **105**, 114010 (2022).
[59] J. Barata, A. V. Sadofyev, and X.-N. Wang, Phys. Rev. D **107**, L051503 (2023).
[60] A. Hebecker, Phys. Rep. **331**, 1 (2000).
[61] J. Casalderrey-Solana and C. A. Salgado, Acta Phys. Pol. B **38**, 3731 (2007).
[62] A. Kovner and U. A. Wiedemann, Phys. Rev. D **64**, 114002 (2001).
[63] Z.-T. Liang, X.-N. Wang, and J. Zhou, Phys. Rev. D **77**, 125010 (2008).
[64] A. Majumder and B. Muller, Phys. Rev. C **77**, 054903 (2008).
[65] Z. Yang, Y. He, W. Chen, W.-Y. Ke, L.-G. Pang, and X.-N. Wang, arXiv:2206.02393.